SAND77-0828
Unlimited Release
UC-66

Geophysical Sensing Experiments On Kilauea Iki Lava Lake

John F. Hermance, Donald W. Forsyth, and John L. Colp

Prepared by Sandia Laboratories, Albuquerque, New Mexico 87185 and Livermore, California 94550 for the United States Department of Energy under Contract DE-AC04-76DP00789

Printed December 1979

Sandia National Laboratories

SAND77-0828
Unlimited Release
Printed December 1979

Distribution
Category UC-66

GEOPHYSICAL SENSING EXPERIMENTS ON KILAUEA IKI LAVA LAKE

John F. Hermance
Donald W. Forsyth
Department of Geological Sciences
Brown University
Providence, RI 02912

John L. Colp
Geothermal Research Division 4743
Sandia National Laboratories
Albuquerque, NM 87185

ABSTRACT

The Hawaiian lava lake in the Kilauea Iki pit crater, resulting from the 1959 summit eruption of Kilauea volcano, has served as a natural laboratory for the continuing study of the petrology, rheology, and thermal history of ponded molten basalt flows in the field environment. During 1975 and 1976, a series of electromagnetic and seismic experiments were coordinated, and in some cases supported, by the Magma Energy Program at Sandia Laboratories in an attempt to define the in-situ geophysical properties and the configuration of the molten lava core as closely as possible. This effort involved workers from the United States Geological Survey (USGS), University of Texas, Massachusetts Institute of Technology (MIT), Sandia Laboratories, and Brown University. Drilling and geophysical experiments in 1976 suggested that the solidified crust of the lava lake had a cool, resistive surface layer, undersaturated with water to a depth of 5 metres. A warm, wet layer containing appreciable water and/or steam was essentially isothermal (100°C) to 33 metres. From 33 to 45 metres the temperature climbed rapidly (from 100° to 1,070°C) until a thin plexus of molten sills was encountered, interbedded with solid layers. Below this (50 metres) was apparently a layer having the highest temperature, lowest viscosity, and lowest density of olivine phenocrysts. At 70 metres, a transition zone to a crystalline mush was indicated, and finally (between 80 and 95 metres), solid basalt extended down to the preflow surface at a depth of 115 to 120 metres.

CONTENTS

ILLUSTRATIONS

ILLUSTRATIONS (Continued)

TABLES

*Aki, K., B. Chouet, M. Fehler, G. Zandt, R. Koyanagi, J. Colp, and R. G. Hay, Journal of Geophysical Research, Volume 83, pp 2273-2282, 1978. Copyright by American Geophysical Union. Used by permission.

GEOPHYSICAL SENSING EXPERIMENTS ON KILAUEA IKI LAVA LAKE

Introduction

In direct response to recommendations made at the Magma Workshop held at Kailua/Kona, Hawaii, 3 to 6 March 1975, (Sandia Laboratories Report, SAND75-0306) the Sandia Magma Energy Project, in collaboration with the United States Geologic Survey (USGS), supported a series of geophysical sensing experiments during 1976 on Kilauea Iki lava lake. A persistent theme throughout the Magma Workshop was discussion on developing and testing techniques for detecting and evaluating the physical and chemical characteristics of major magma structures at depth within the earth's crust. As a result, a recommendation was made to test various geophysical techniques on known magma bodies such as Kilauea Iki so that the effectiveness of the different methods could be determined.

A parallel recommendation of the workshop was to use geologic information from eroded and exhumed fossil magma systems to better understand present-day active magma systems.

Both of these recommendations have resulted in a comprehensive investigation of the configuration and physical characteristics of a known small-scale magma system in Kilauea Iki crater on the island of Hawaii.

The lava lake in the Kilauea Iki pit crater resulted from the summit eruption of Kilauea volcano (Figure 1) during November and December 1959. The Kilauea Iki pit crater was approximately 200 metres deep before the eruption. On 14 November 1959, a fissure opened halfway up the southwest wall of the crater, and lava flowing from the fissure quickly filled the pit crater to the level of the eruption vent during a single eruptive phase lasting 7 days (Figure 2, this report; Richter et al, 1970, p E5). The total lava erupted during this first phase has been estimated at 40×10^6 cubic yards. During the month following, 16 additional discrete sequences of lava outpouring and draining back into the vent added approximately another 10×10^6 cubic yards to the volume of the molten lava pond. By 20 December 1959, activity ceased; the level of the lake stood 110 to 120 metres above the original floor, and the lake had a diameter of approximately 750 metres. See Figure 3 (measurements are in feet).

Additional lava lakes have formed since 1959 along the east rift of Kilauea: Aloi (1962, 1965), Alae (1963, 1968), and Makaopuhi (1965), although at present only Kilauea Iki is accessible, the others having been covered by the eruption of 1969 and later (Wright et al, 1976).

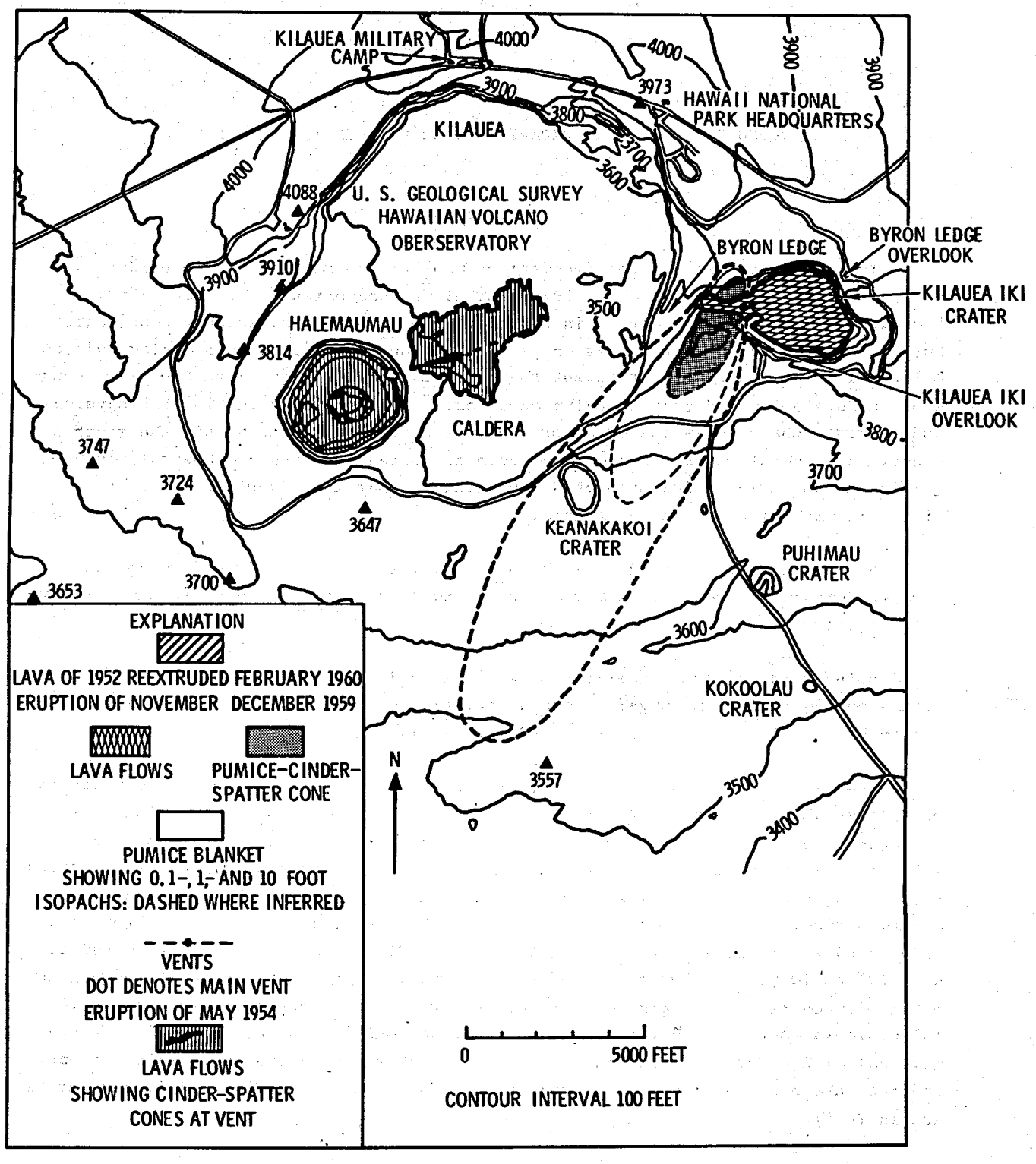

igure 1. Map of the Kilauea Summit Area, Showing Principal 1959 Eruptive Features in and around Kilauea Iki and the 1960 Collapse in Halemaumau. Location of outline and vents of the 1954 flow on the caldera floor are from MacDonald and Eaton, 1957 (after Richter et al, 1970, Figure 3).

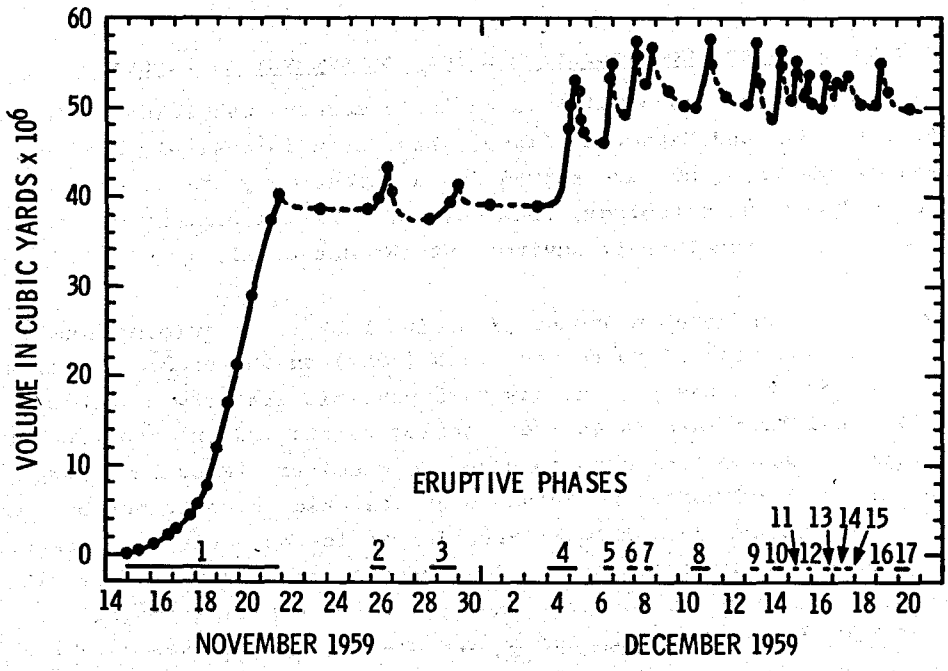

Figure 2. Graph Showing Volume of Lava Erupted into Kilauea Iki during the 1959 Summit Eruption. Dashed line after the end of an eruptive phase represents backflow of lava down the vent. Each dot is a volume measurement. Note that the volume of total lava actually decreased during the fourth eruptive phase (after Richter et al, 1970, Figure 2).

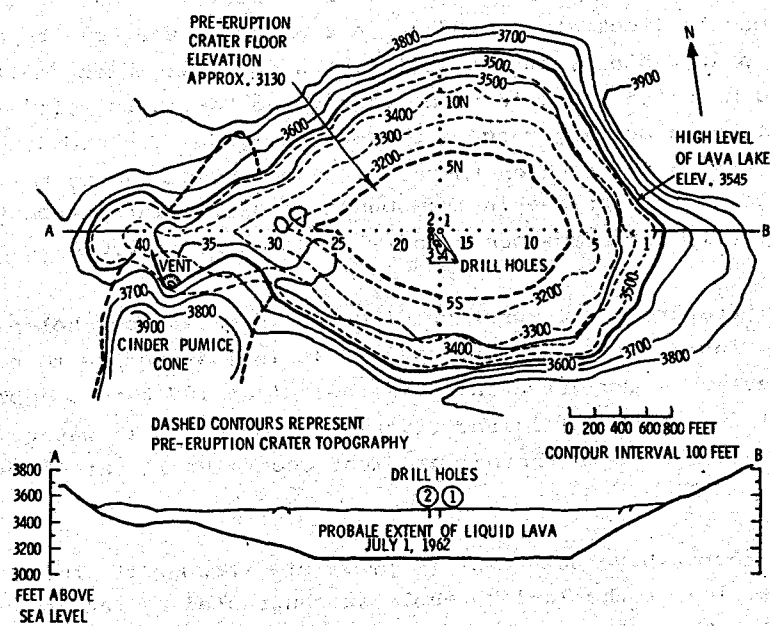

Figure 3. Map and Section of Kilauea Iki Crater before and after the 1959 Summit Eruption, Showing Location of USGS Drill Holes. Small open circles show location of permanent reference stations on the lava lake (after Richter and Moore, 1966, Figure 2).

Constraints on Lava Lens Configuration Prior to Geophysical Experiments

Because of their accessibility, the three modern lava lakes, Kilauea Iki (1959), Alae (1962), and Makaopuhi (1965), have been intensively drilled, cored, and sampled by the USGS and have served for a number of years as natural laboratories for studying the petrology, rheology, and thermal history of ponded molten basalt flows in the actual field environment (Wright et al, 1976).

Moreover, a considerable amount of useful background information has been supplied through the work of Moore and Evans (1967) on the exposed, prehistoric lava lake revealed when the present day Makaopuhi pit crater was formed. The prehistoric Makaopuhi lava lake is an ideal analog to the modern lava lakes because of its similarity to the modern lakes in size and chemistry (Moore and Evans, 1967). In a sense, the work of Moore and Evans is as essential a contribution to the interpretation of geophysical data from Kilauea Iki as is the study of exhumed fossil plutons to geophysical measurements of deep crustal magma structures. It was logical, therefore, that the Sandia Magma Energy Project mobilize its efforts around the knowledge of both the prehistoric and modern Hawaiian lava lakes established through the long-term research activities of the USGS.

The most fundamental constraint on the present configuration of Kilauea Iki lava lake is the present total thickness of the lava flow, both chilled and molten, of 115 to 120 metres (Holcomb, 1976). Since 1960, 55 holes have been drilled through the crusts of the 3 lava lakes (13 of which were drilled through the crust of Kilauea Iki lava lake (Colp and Okamura, 1978)). Temperatures logged in these holes, as well as total crustal thicknesses, are useful in constructing and testing thermal history models (Peck et al, 1977). A summary of the results of the Kilauea Iki holes is given in Table 1, in particular, the depth at which "melt" was encountered. It should be noted, that in this regard, the "depth to melt" is a pragmatic term since basalt has a melting range from 980° to 1,200°C. According to Wright et al (1976), it is the depth at which there is a marked decrease in the rigidity of the basalt as well as an increase in the abundance of olivine phenocrysts. This so-called liquid/solid interface occurs at a temperature of 1,070 $\pm$ 5°C.

Typical temperatures as a function of depth in recent boreholes on Kilauea Iki are given in Figure 4 (after Colp, 1976). It is instructive to note in this figure that temperatures are essentially isothermal at 100°C to a depth of 33 metres (110 feet) due to the efficient circulation of meteoric water. From 33 to 45 metres, a sharp increase in thermal gradient occurs until, at 45 metres, melt is encountered.

Very few attempts have been made to penetrate through the melt, but this was the specific objective of the 76-1 borehole subcontracted by Sandia and supervised by USGS personnel. This hole encountered melt at 44.7 metres, and, when an attempt was made to push through the melt, progress was stopped by a rigid obstacle at 45.3 metres. In other words, only 0.5 metre of melt was penetrated. This fact has raised three possibilities regarding the drilling results: (1) the actual molten lava lens is only a half metre thick, (2) a thin zone or plexus of molten sills is an inherent feature of the cooling process (a possibility favored by Colp and

Table 1

Sequence of Holes Drilled into Kilauea Iki (after Colp and Okamura, 1978)

Drilling Agency	Date	Number of Holes 1-3/16-in. dia.	2-in. dia.	3-in. dia.	Depth to Melt (ft)
HVO	4-8/1960	1			16.0
LRL	7/1960		1		19.0
HVO	4/1961	1			29.7
HVO*	10/1961				35.0
HVO	5-6/1962	1			41.6
HVO	12/1962	1			43.6
HVO	3/1967			1	85.0
HVO	5-7/1967			1	85.0
HVO	10/1967			1	87.0
HVO	2-3/1975			3	145.0
SANDIA/HVO	8/1976			2	149.3

*Redrilled and deepened hole originally in April 1961.

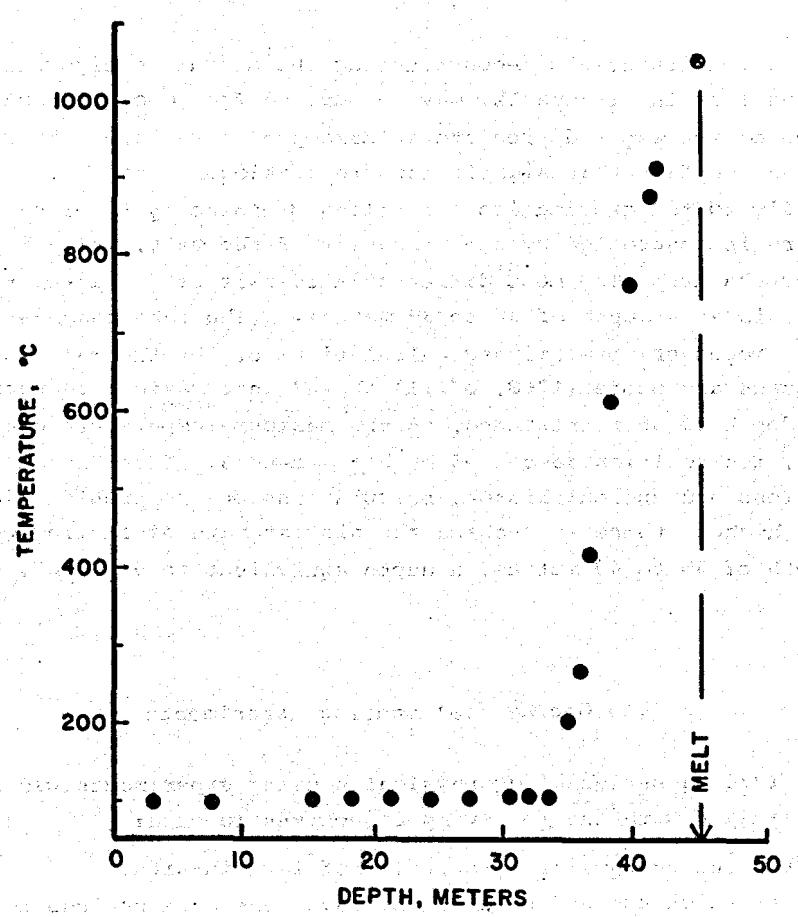

Figure 4. Kilauea Iki Borehole Temperature Profile (after Colp, 1976)

Okamura, 1978), or (3) the drill did indeed hit the principal molten lens and then struck a piece of foundered, more refractory material, such as a piece of stopped crust.

It will be shown that the geophysical measurements have detected a molten lens from 15 to 30 metres thick, which appears to rule out the first possibility (above). On the other hand, the second possibility is very real, particularly in view of the observation by Peck et al (1977, p 429) that a preliminary calculation of the thermal history of Kilauea Iki lava lake by Tom Wright suggested a crust that in January 1975 should have been approximately 58 metres thick. Table 1 shows that this was at variance with the actual observation of 43 to 44 metres in holes drilled in February 1975. Peck et al (1977) suggest that a possible reason for this may be that the effect of rain water is less for cooling thick flows than thin flows because, in thick flows, some of the flashed steam is condensed before it reaches the atmosphere and is recycled within the chilled basalt column without effectively transferring heat to the free atmosphere. Alternatively, Peck et al may have underestimated the depth to the actual molten lens because they too have encountered the plexus of sills that the 76-1 borehole encountered. Undoubtedly, rain water is less effective in transferring heat in thick than in thin flows, but the molten core of the lava lens may be somewhat deeper than indicated by the uppermost melt accumulation.

Additional constraints on reconstructing the actual configuration of the present-day lava lens in Kilauea Iki may be imposed from geologic and thermal history studies of the exposed prehistoric Makaopuhi lava lake. Moore and Evans (1976) have used the fact that significant fluctuations in the bulk rock chemistry are due primarily to the gravitational settling of phenocrysts of olivine; this settling in turn is controlled by the viscosity of the melt, which is a strong function of temperature. The most differentiated part of the lake, the olivine-depleted layer, is at a depth of 30 to 39 metres. (The lake reaches a total depth of 63 metres.) Moreover, preliminary calculations of the thermal history of this same lake by Evans and Moore (1968, p 111) showed that maximum temperatures were attained at a depth of 36 metres, and, as the maximum temperature decreased in time due to cooling, its position descended by 5 $\pm$ 3 metres. Thus, according to the field observations and thermal history calculations on the prehistoric Makaopuhi lava lake, the highest temperatures and the slowest rate of cooling were experienced at a depth of 36 to 40 metres, a depth equivalent to 54 to 60% of its total thickness.

The Geophysical Sensing Experiments

In early 1976, a series of geophysical sensing experiments was initiated on Kilauea Iki lava lake with the following objectives in mind:

1. Monitor the geophysical properties of lava in-situ,
2. Map the thickness and edge of the lava lens as a prelude to an extensive drilling program, and

3. Evaluate the feasibility of using geophysical methods for detecting and delineating major magma structures in the earth's crust (2 to 10 km).

Both seismic and electromagnetic experiments were carried out by a number of people from Sandia Laboratories, the USGS, MIT, and the University of Texas at Austin. Table 2 provides a list of the types of experiments carried out.

Table 2

Geophysical Experiments Performed
On Kilauea Iki Lava Lake

1. Dipole-Dipole Electromagnetic Induction Experiments (Frischknect, Zablocki, B. Smith, Flanigan)
2. Very-Low-Frequency Radio Wave Methods (Zablocki, Anderson)
3. Galvanic Four-Electrode Resistivity Soundings (Zablocki, B. Smith)
4. Audio-Frequency Magnetotelluric Profiling And Sounding (Bostick, S. Smith, Boehl)
5. Passive Monitoring of Seismic Noise (Aki, Chouet, Colp)
6. Teleseismic Measurements (Aki, Chouet)
7. Small-Scale Seismic Refraction Experiments Using Artificial Charges (Aki, Chouet)

Active Electromagnetic Experiments

The interpretation of the active electromagnetic experiments has led to quantitative estimates of the depth, thickness, and lateral dimensions of the lava lens. It is worth reexamining the uncertainties and assumptions involved in the interpretation because a number of the conclusions are in direct conflict with the reported results of the seismic experiments. The following discussion separates the suite of active electromagnetic experiments into two groups, those defining the vertical structure and those defining the lateral boundaries of the lava lens.

Vertical Sounding -- Two classes of electrical experiments were carried out to study the vertical structure of the lava lens. Zablocki (1976) describes Schlumberger, or galvanic, four-electrode electrical sounding data obtained from expanding the separation between electrodes along the two lines indicated in Figure 5, VES-NS and VES-EW (VES: Vertical Electrical Sounding). During the spring of 1976, two-loop electromagnetic soundings were performed by the USGS, using a transmitting loop located as shown in Figure 5 and receiving loops placed first 108 metres and then 200 metres from the center of the transmitter loop.

The Schlumberger (Galvanic) Soundings -- The Schlumberger data of Zablocki (1976) shown in Figure 6 has contributed significantly to defining the vertical structure of the chilled resistive layers above the molten lava lens. According to Zablocki (1976), the surface layers have the configuration indicated in Table 3.

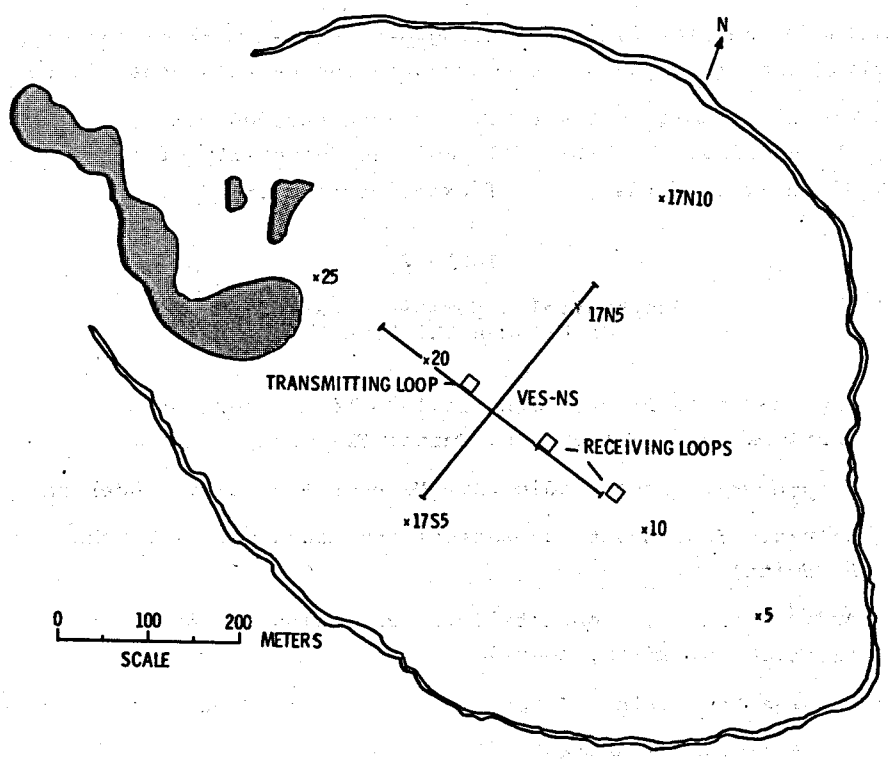

Figure 5. Location of Vertical Electrical Sounding Lines in Kilauea Iki Crater (after Smith et al, 1977, Figure 1)

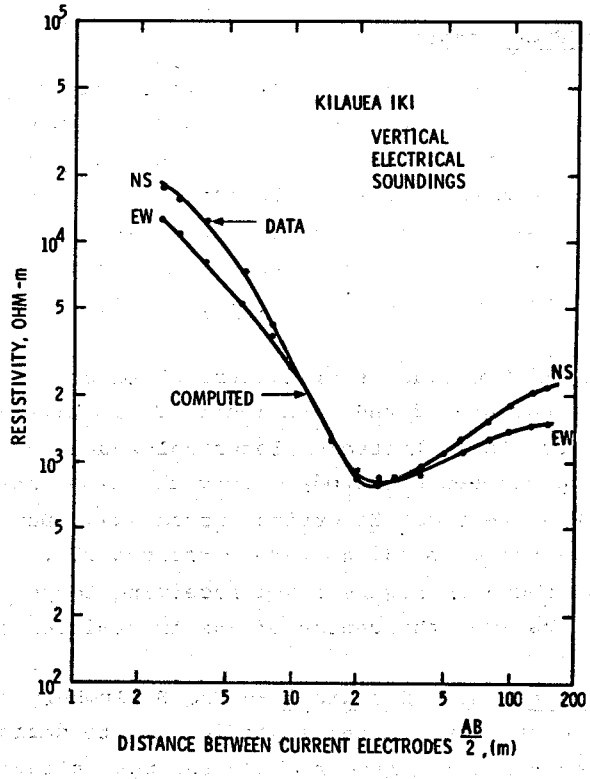

Figure 6. Kilauea Iki VES. Computed curves are for the range of parameters summarized in Table 3 (after Smith et al, 1977, Figure 5).

Table 3

Interpretation of Schlumberger Data (after Zablocki, 1976, and Smith et al, 1977)

Layer Number	Depth to Top (metres)	Resistivity (ohm-metres)
1	0	25,000
2	1.0 - 1.7	5,000 - 7,000
3	4.0 - 5.4	600
4	33	(40,000?)
5	(44?)	(3?)

The high resistivity of Layer 1 is undoubtedly due to a low concentration of pore fluids (meteoric water) in a very porous and heavily fractured material. The somewhat lower resistivity of Layers 2 and 3 may reflect a higher pore fluid concentration, along with an increase in the amount of dissolved salts in the fluid due to its recycling in a fairly active convection zone.

The value of resistivity for Layer 4 is undoubtedly large, and 40 000 ohm-metre could easily be a minimum value. Zablocki (1976) has stressed that the thickness of Layer 4 and the resistivity of Layer 5 as indicated in Table 3 are possible interpretations only. These parameters are not well defined by the Schlumberger data alone. On the other hand, the two-loop electromagnetic induction measurements by Smith et al (1977) significantly constrain the interpretation of these deeper layers.

The Electromagnetic (Two-Loop) Soundings -- During the spring of 1976, Smith et al (1977) carried out a two-loop electromagnetic sounding over the approximate center of the lava lens at two fixed transmitter-receiver spacings, 108 and 200 metres. Their results are summarized in Table 4. Several layer parameters were constrained by Smith et al in their least-squares inversion of the electromagnetic data: the resistivity and thickness of the first layer (reasonably well known from the Schlumberger measurements), the thickness of the second layer (assumed to be a warm wet layer), and the resistivity of the third layer.

The resistivity of the melt layer (Layer 4) was expected to have the value determined from a previous loop-loop electromagnectic sounding performed in 1962, when the crust of the lake was only 13 metres thick. Since it is not clear whether the melt resistivity has changed appreciably over the ensuing 14 years, 2.3 ohm-metres may represent a lower limit on the present-day resistivity. What little laboratory data are available on the electrical conductivity of basalt over its melting range, 980°C to 1,200°C, suggests that the electrical conductivity changes drastically in passing from the liquid to the solid state. A conservative estimate based on data from Presnall et al (1972) and Khitarov and Sluitskiy (1965) is a change of 3%/°C in the vicinity of 1,150°C. Murase and McBirney (1973) present data for tholeiitic basalt leading to a value of 2.25%/°C. However, over a limited temperature range, the laboratory data of Presnall et al (1972) show a change as great as 100%/°C, or a total change from 1,200°C to 1,100°C of two orders of magnitude! However, this is very likely an extreme value, and variations of, say, 3%/°C in the vicinity of 1,150°C are more likely to be encountered.

Table 4

Combined Interpretation of Geoelectric Section Using Schlumberger and Loop-loop Electromagnetic Sounding (after Smith et al, 1977)

Layer Number	Depth to Top (metres)	Resistivity (ohm-metres)
1	0	25,000
2	4.5	300 to 750
3	28	10 000 (min)
4	32.3 to 44.4	2.3
5	49.8 to 60.1	10 000 (min)

Smith et al note that the electromagnetic soundings cannot resolve the resistivity and the thickness of the lava lens separately; however, the conductivity-thickness product (the conductance) of the melt layer is well determined and has a value of 7.64 mhos from the 108-metre sounding. The value of 6.86 mhos for the conductance of the lava lens from the 200-metre sounding may be biased toward somewhat lower values by either the finite geometry of the lava lens or by lateral changes in the lava lens itself (Smith et al, 1977).

Although the USGS interpretation advocates a thickness of 17.5 metres for the lava lens, this is true only if the resistivity of the melt has not changed since it was determined originally in 1962. As mentioned above, if the melt has cooled 30°C, then the resistivity would increase by a factor of 2, and, for the same layer conductance, a thickness of 35 metres would be required. While the interpretation is apparently better constrained than this, the possibility that an ambiguity of this magnitude for layer thickness should not be unexpected has also been pointed out by Frischknect (1976).

A schematic of a conceptual model proposed by Smith et al to account for the essential elements of the Schlumberger and two-loop electromagnetic sounding experiments is presented in Figure 7. The Schlumberger data have quite adequately defined the presence of (1) a relatively dry surface layer, (2) a warm wet conductive layer (300 to 700 ohm-metres), and (3) a dry resistive layer (on the order of 40,000 ohm-metres) in which temperatures are sufficiently high to drive off significant amounts of water vapor. The two-loop electromagnetic measurements have also defined (4) a conductive melt, 17.5 metres thick, having a resistivity of 2.3 ohm-metres, and (5) a dry resistive layer below.

In order to reconcile the electromagnetic interpretation with the drilling results and thermal modelling estimates, Smith et al present the geological model shown in Figure 8. The top of the principal molten lava lens is pegged to the depth at which drilling encountered "melt." The fact that the Sandia Laboratories

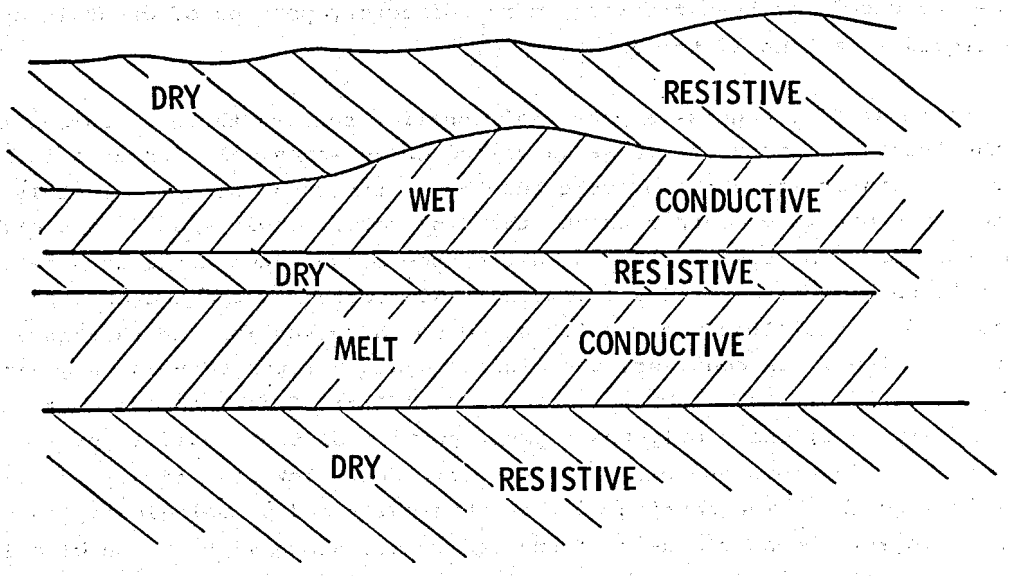

Figure 7. Conceptual Model of Kilauea Iki Lava Lake (after Smith et al, 1977, Figure 4)

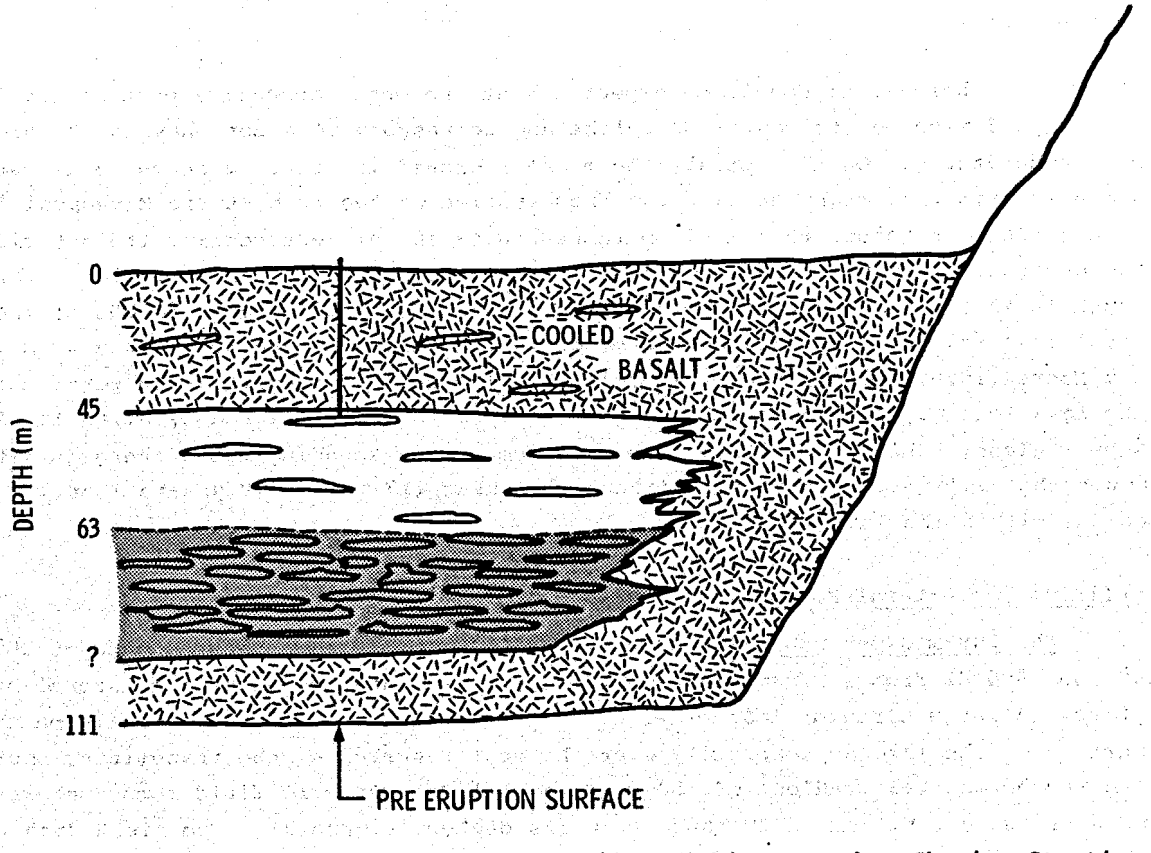

Figure 8. Complex Geological Model of Kilauea Iki Lava Lake, Showing Stratification in the Melt Zone. The lower shaded zone is less conductive than the upper, not shaded, zone (after Smith et al, 1977, Figure 14).

hole KI 76-1 penetrated only 0.5 metre of liquid before encountering an obstacle may be accounted for by a floating, more refractory portion of crust in an otherwise liquid lava lens 17 to 18 metres thick.

Smith et al recognize a potential conflict between the electromagnetic model and the thermal history estimates described above which call for a ratio between the cooling rates for the top crust and the bottom crust of approximately 60/40. If the top crust is 45 metres thick, then the bottom crust should be two-thirds of 45 metres, or 30 metres thick. The difference between the total lava lake thickness (115 to 120 metres) and the combined thicknesses of the two chilled crusts (30 metres + 45 metres) leads to a value of 40 to 45 metres for the thickness of the liquid lava lens. In contrast, the electromagnetic interpretation suggested a thickness of 17.5 metres. To resolve this conflict, Smith et al suggest the model shown in Figure 8, where only the topmost portion of the liquid layer is "electrically active" in the sense of having a sufficiently low resistivity to differentiate it from the lower portion of what physically and petrologically is still a "liquid" layer. Dense blocks of foundered crust, along with a mush of olivine phenocrysts collecting on the bottom of the molten liquid layer due to gravitational settling, will serve to increase the resistivity sufficiently to neutralize the conductance of this portion of the liquid layer. This is a very plausible explanation and indicates that caution should be used in expecting a one-to-one correspondence between the electrically active layer and the petrological/rheological molten layer.

Nevertheless, it should be expected that the most conductive part of the lava lens should also be its most liquid-like and correspond to a zone having the highest temperatures. On this point, the model proposed in Figure 8 seems to differ slightly from what might be expected from studies on the prehistoric Makaopuhi lava lake since it suggests that maximum temperatures and slowest cooling (to get rid of the crystalline mush) is at a depth of 45 to 63 metres, or, say, 55 metres. This depth is 45 to 50% of the total lake thickness as compared with 55 to 60% of the total lake thickness based upon the prehistoric Makaopuhi lava lake study of Evans and Moore (1968). In short, it is felt that the active or most liquid portion of the lava lens may be somewhat thicker and deeper than is inferred by Smith et al. Nevertheless, based on the loop-loop electromagnetic sounding data, there is little doubt that a liquid core of significant thickness (17 metres or greater) still exists within the lava lake.

Defining the Lateral Boundaries

The Turam Experiment -- Flanigan and Zablocki (1977) have used data at 200, 400, and 800 Hz from a Turam experiment on the lava lake to define its lateral boundaries. A large circular loop of wire (100-metre diameter) placed directly on the surface of the lake approximately over the center served as the transmitter source, and the horizontal gradient of the complex vertical magnetic field component was measured as a function of distance from its center (Figure 9). The field data were then compared with a small analog scale model in the laboratory (Figure 10). Melt conductivity and thickness were inferred from the studies of Smith et al (1977), and the depth to the melt was predicted on the basis of the drilling results (Colp and

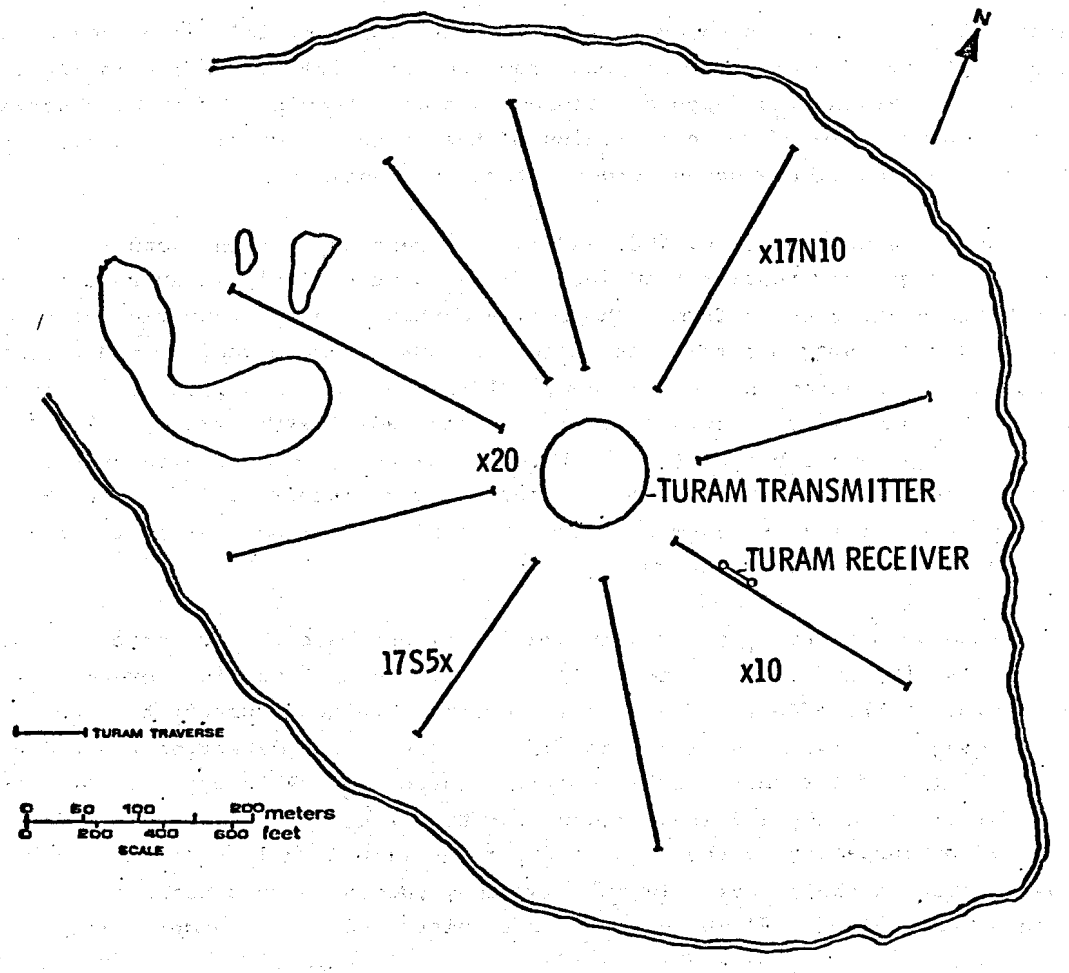

Figure 9. Location of Turam Transmitter and Measurement Array on Kilauea Iki Lava Lake (after Flanigan and Zablocki, 1977, Figure 1)

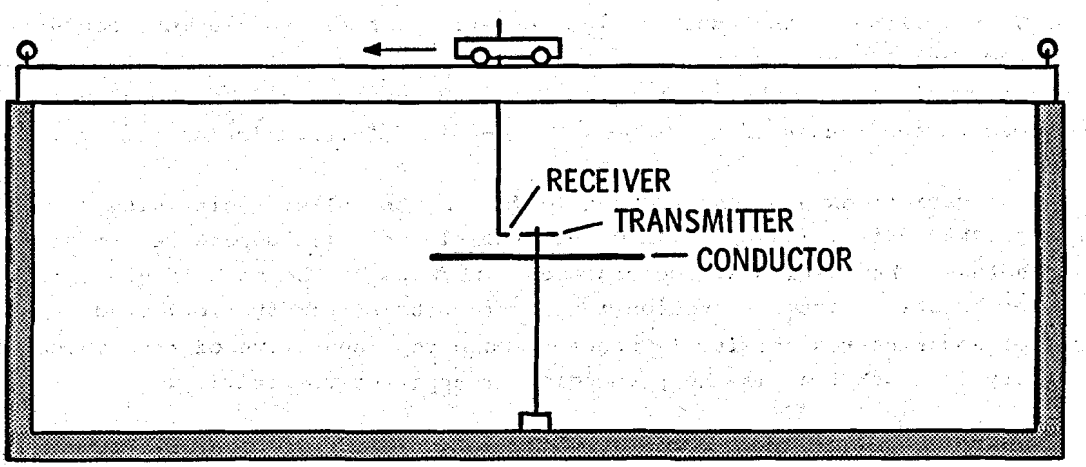

Figure 10. Schematic of Analog Scale Model Tank Setup in Laboratory (after Flanigan and Zablocki, 1977, Figure 5)

Okamura, 1978). Although the possibility exists that any inference regarding the location of the edge of the melt zone from the Turam interpretation is inbred with inferences regarding its depth and conductance as determined by other observations, for the aspect ratio of depth to radius of the structure considered here, these uncertainties contribute second order effects at most.

Three frequencies (200, 400, and 800 Hz) were used in the actual field experiment, although only results from 400 Hz were quantitatively interpreted. The variation between the results from each profile contoured on a plane view of the lava lake (Figure 11) suggests that the target is somewhat more complicated than a homogeneous lens implanted in a homogeneous half-space. A comparison of the normalized field ratios among the various profiles shows a radial asymmetry of 10%. As pointed out by Flanigan and Zablocki (1977), this asymmetry could be caused by (1) differences in the conductivity thickness product (layer conductance), (2) depth to the molten basalt, or (3) the asymmetric position of the transmitter coil relative to the edges of the molten lava lens.

Although a relatively broad spread is evident when they compare the data from all profiles (Figure 11), Flanigan and Zablocki use a clever interpretational device that minimizes the effects of such a large spread between curves; they use the data along a single radial direction from the transmitter and determine the radius of the best-fitting disk for that single profile (Figure 12). Although data from the next radial give a slightly different radius for the disk, they treat this difference as an actual perturbation of the edge of the conducting lava lens, rather than an intrinsic error in their data. In this way they successfully construct an outline of the lava lens (Figure 13) which is somewhat distorted from a simple disk.

The Very Low Frequency (VLF) Experiment -- Preliminary magnetotelluric profiling at very low frequencies (VLF), 23.4 kHz and 18.6 kHz, presented by Flanigan and Zablocki (1977), shows dramatic increases in apparent resistivity near the edges of the melt zone (Figure 13). Apparent resistivities are quite low over the lens itself, but, close to the edge, a high-resistivity zone, then a more conductive zone, and finally another high-resistivity zone are encountered. These variations are most prominent for the apparent resistivity determined from the electric field polarized perpendicular to the edge, the so-called "perpendicular resistivity."

The variations are less pronounced for the "parallel resistivity," which is the apparent resistivity determined from the electric field parallel to strike, but, nevertheless, the results are consistent. In fact, at the high frequencies and their associated short attenuation lengths (depths of penetration) used here, the parallel apparent resistivity is probably more representative of true value of resistivity at depth than is the perpendicular apparent resistivity.

The authors note the smooth flat behavior of apparent resistivities over the interior of the lava lake and point out that one-dimensional models fitting the VLF apparent resistivity data over the center of the lake require the presence of a low resistivity layer (120 ohm metres) above the molten lens, underlaid by a zone of

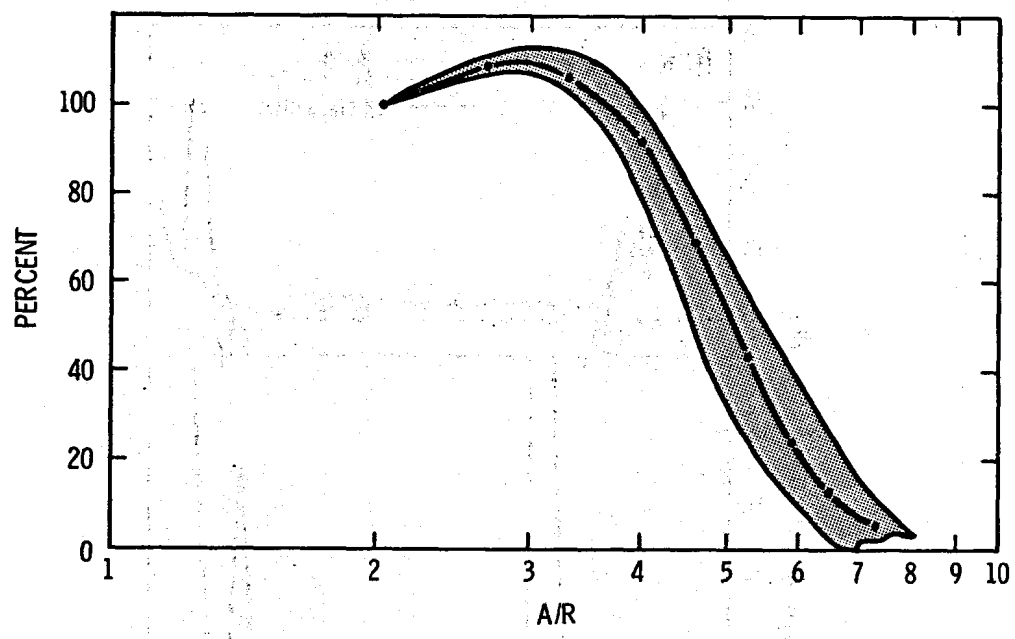

Figure 11. Real Component of the Electromagnetic Field, Kilauea Iki Lava Lake. The ordinate is in percent of field from an arbitrary point. The abscissa is the ratio of A/R, where A is the distance from the center of the transmitting loop to the center of the two receiver loops and R is the radius of the transmitting loop. Shaded region shows the range in the field curves obtained along all nine traverses (after Flanigan and Zablocki, 1977, Figure 3).

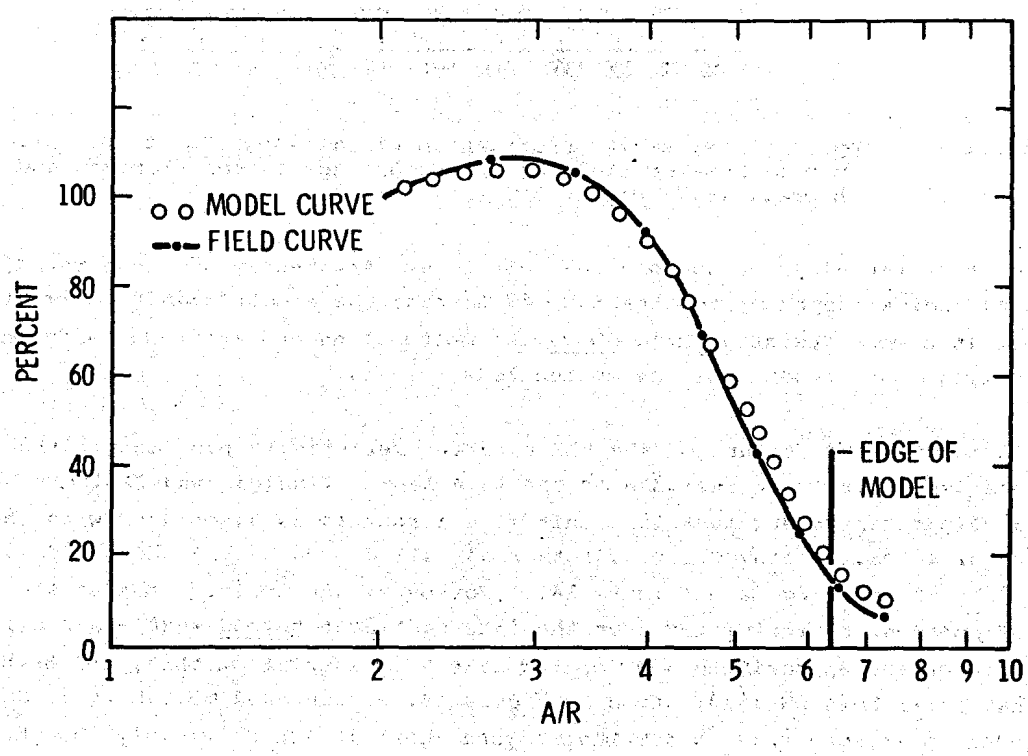

Figure 12. Real Component of a Model Curve (circles) and the Real Component of the East Field Traverse. The edge of the conductive model represents a field distance of 320 metres from the center of the transmitting loop (after Flanigan and Zablocki, 1977, Figure 7).

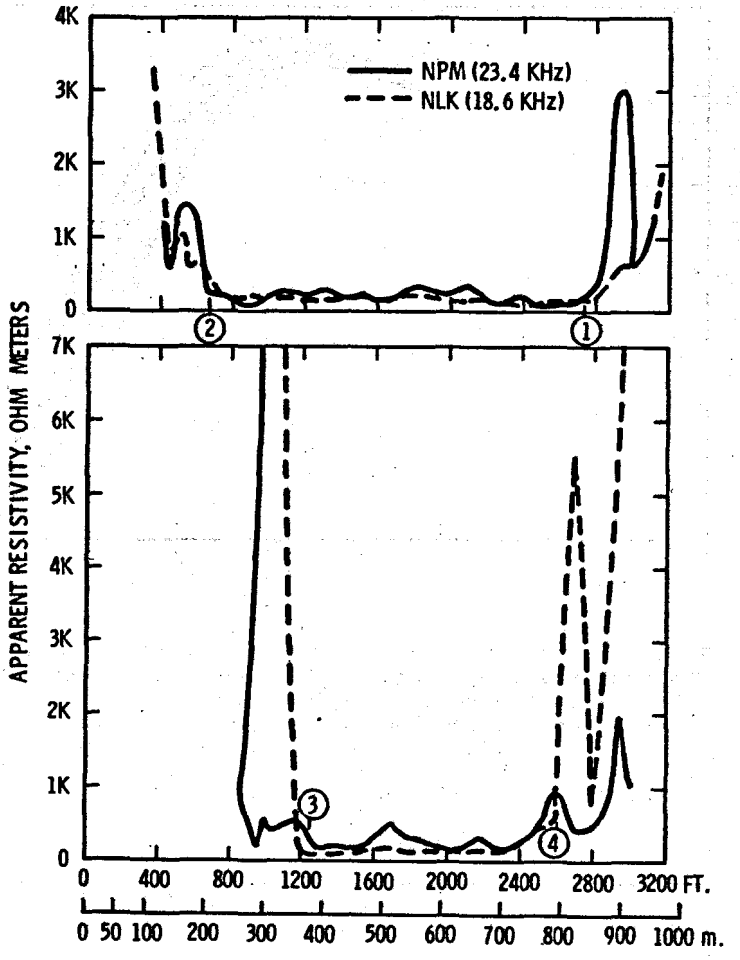

Figure 13. Apparent Resistivity Profiles Obtained Along Traverses. Circled numbers show locations of conductor edge (after Flanigan and Zablocki, 1977, Figure 8).

much lower resistivity, presumably the melt zone. Apparently at these relatively high frequencies (depth of penetration ~40 metres) the electromagnetic fields are absorbed in a more resistive halo above the molten lens and are responding only indirectly to the presence of the molten lens itself.

An interesting feature of the VLF apparent resistivity profiles is the fine structure associated with the edge of the lava lens. Flanigan and Zablocki have advanced a persuasive argument that this fine structure is associated with the presence of a shallow convective hydrothermal cell driven by the thermal energy released by the cooling lava (Figure 14). Moreover, they point out that the flat trend of apparent resistivities over the lake continues beyond what was previously thought to be the approximate edge of the lake. In support of this, the authors note that drill hole DH 75-3, shown in Figure 14, encountered molten lava, so that perhaps the melt zone extends somewhat beyond where it was previously thought to be.

It might be noted in passing that the present temperature inferred at the prefilling crater surface appears to be low compared with the thermal modelling

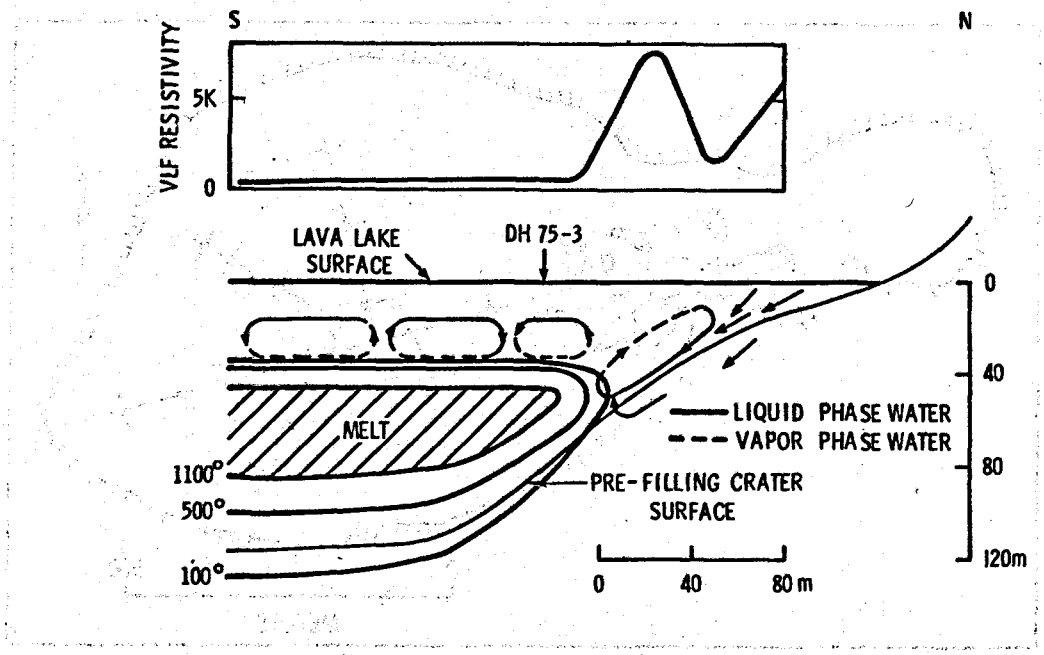

Figure 14. Conceptual Model of the North Edge of the Lava Lake, Showing the Possible Configuration of the Melt Lens, the Hydrothermal System, and Temperature Distribution within the Lake That Might Account for the Generalized Resistivity Profile Shown on Top (after Flanigan and Zablocki, 1977, Figure 9)

estimates by Dallas Peck. Apparently temperatures at this surface should be expected to stabilize at values as high as 700°C for a considerable portion of the lifetime of the molten lens; this is higher than the value of 200° to 300°C indicated in Figure 14.

Audio Magnetotelluric Measurements

During May 1976, the Electrical Geophysics Laboratory of the University of Texas, Austin, performed audio magnetotelluric measurements at 20 sites in Kilauea Iki crater (Figure 15), as well as 6 other sites over the summit of Kilauea volcano (Bostick et al, 1977). These measurements gave rather unexpected results and in retrospect demonstrate two things:

1. The interpretation of magnetotelluric measurements in three-dimensional situations is sometimes not a simple extension of one- or even two-dimensional theory and
2. Magnetotelluric data, even under relatively complicated field conditions, when properly interpreted can lead to insight regarding the target that is not attainable from other measurements.

To illustrate the first point, Bostick et al calculated, as part of a pre-field planning exercise, the plane-layered (one-dimensional) magnetotelluric response for the layer parameters given in Table 5. These estimated values were based on electromagnetic work as well as on thermal modelling calculations performed previously by USGS workers.

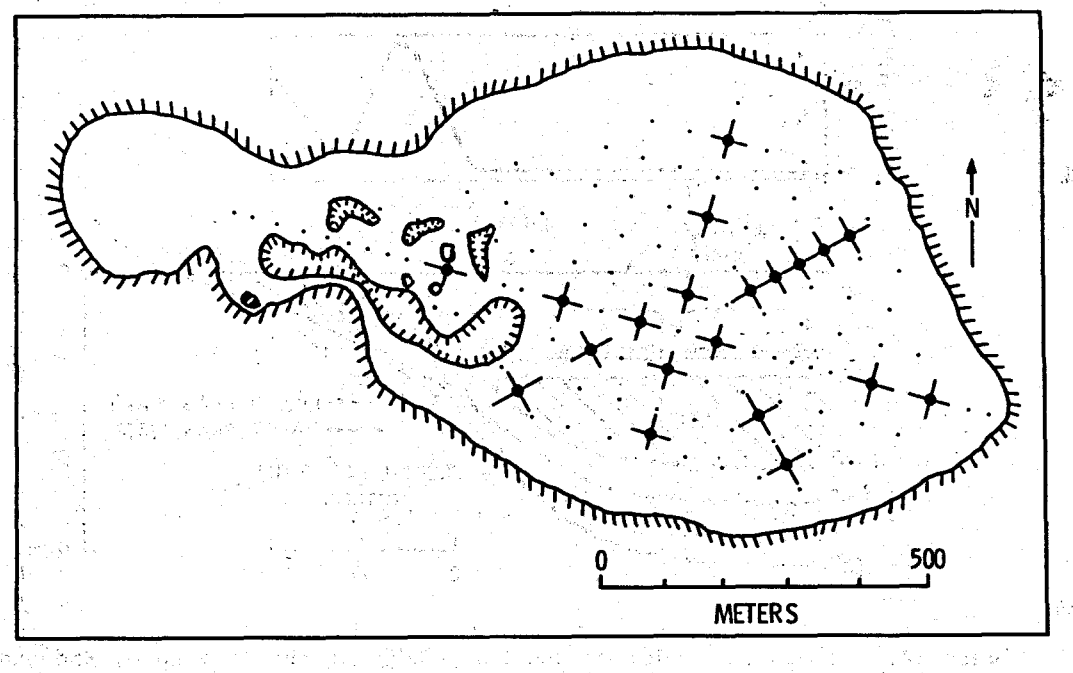

Figure 15. Location of Audio-Magnetotelluric Sites on Kilauea Iki Lava Lake (after Bostick et al, 1977)

Table 5

Plane-layered Model to Simulate Lava Lake (Bostick, Smith and Boehl, 1977).

Layer Number	Depth to Top (feet)	True Resistivity (ohm-metres)
1	0	1,000
2	150	2
3	225	1,000

However, as it turned out, the observed data (Figure 16) looked very little like the expected plane-layered response calculated prior to the field program. The most striking difference is the fact that the parabolic-shaped minimum in the theoretical curve caused by the lava lens is clearly absent in the field data. This apparently is due to the effects from the finite size of the lava lens. Based upon magnetotelluric data only from sites over the middle of the lava lake and upon experience with plane-layered interpretations, the assertion that a lens-like conductor was present would likely not have been made. However, since both drilling and the active electromagnetic sounding experiments indicate molten material at a depth of only 40 to 45 metres, the lava lens does exist.

In order to model the possible effect of the finite geometry of the lava lens, Bostick et al assume that their lowest frequency, 17 Hz, is of a sufficiently long period that induction effects can be neglected and then model the response of the lava lens simply as the distortion of a uniform dc-telluric field by an imbedded

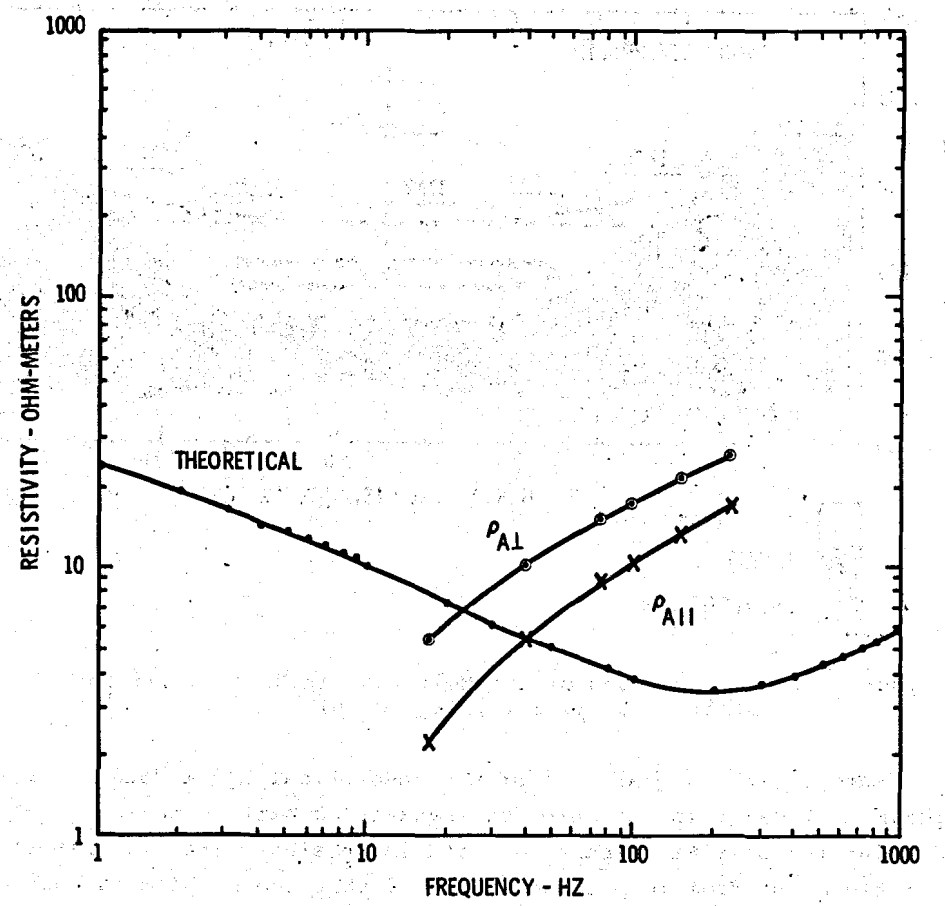

Figure 16. Observed Apparent Resistivities Compared with the Theoretical Response of a Plane-Layered Model Having the Characteristics Given in Table 5 (after Bostick et al, 1977)

conducting inhomogeneity. A series of straightforward, though approximate, corrections accounts for the fact that the lava lens is beneath the floor of a crater-type structure, and the final model they consider is shown in Figure 17.

The smooth curves in Figure 18 represent theoretical magnetotelluric apparent resistivities "normalized" to values away from the crater disturbance, for various thicknesses of the lava lens in metres. The apparent resistivities are calculated for the electric field perpendicular to the edge of the melt and parallel to the edge of the melt. It should be noted that the curves for a given melt thickness show the greatest separation near the edge of the melt zone; whereas, over the center of the lens, the theoretical curves from the two polarizations should come together for each model. In fact, this does not seem to happen in the real data, which are shown as the points in Figure 18 where the true distance of each site from 17N2 is normalized by the radius of the lava lens (275 metres) assumed by Bostick

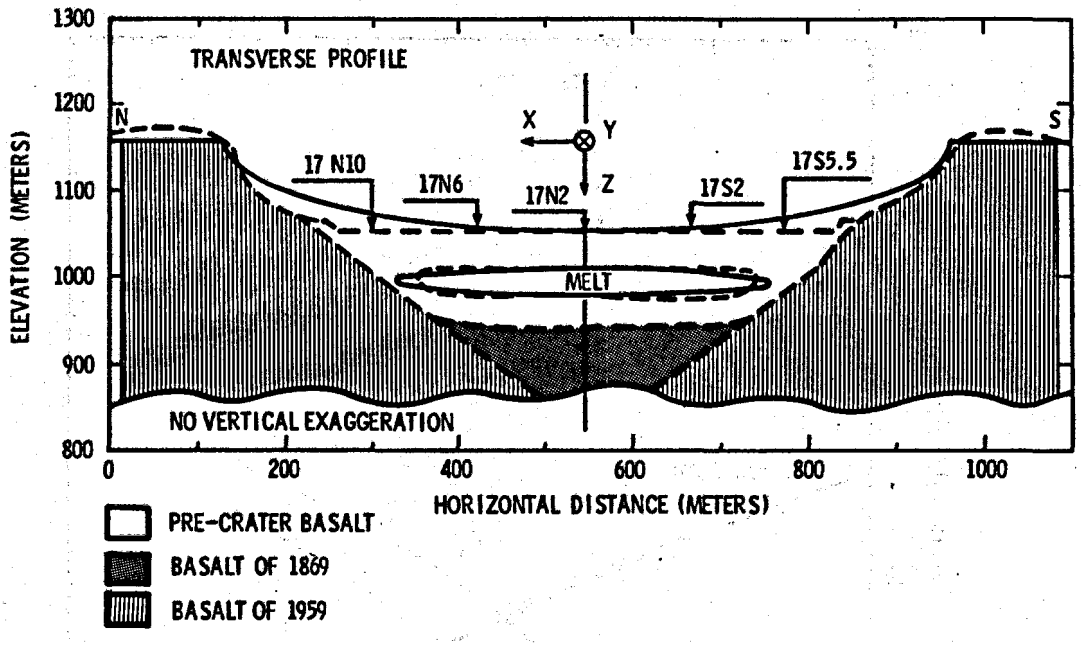

Figure 17. Assumed Form of the Melt Zone in Kilauea Iki Lava Lake (after Bostick et al, 1977, Figure 10)

et al. Clearly, certain qualities of the theoretical model data are reflected in the experimental data; for example, the separation between the parallel and perpendicular resistivities increases with increasing distance. Nevertheless, there can be little doubt from inspecting Figure 18 that the problem is much more complicated than the simple model used in the interpretation; particularly, the observed principal resistivity values over the center of the lake do not come together as suggested by the model.

Bostick et al note that the observed minimum in apparent resistivity over the center of the lava lake (site 17N2) is compatible with a lens thickness of approximately 4.6 metres, which gives a conductance for the lens of 2 mhos, much less than the 6.9 to 7.6 mhos determined by Smith et al (1977) using the two-loop electromagnetic sounding method. To explain this discrepancy, Bostick et al have invoked the possible effect of a resistive "steam" sheath surrounding the lava lens. Using Schlumberger soundings, Zablocki (1976) has apparently detected such a zone directly above the lava lens. If such a zone completely surrounds the lens, it undoubtedly represents a very high resistance in series with the conducting lens. The net effect would be to decrease the apparent conductance that would be inferred from surface telluric measurements, perhaps enough to reduce the apparent conductance from 7 mhos to 2 mhos (Bostick et al, 1977).

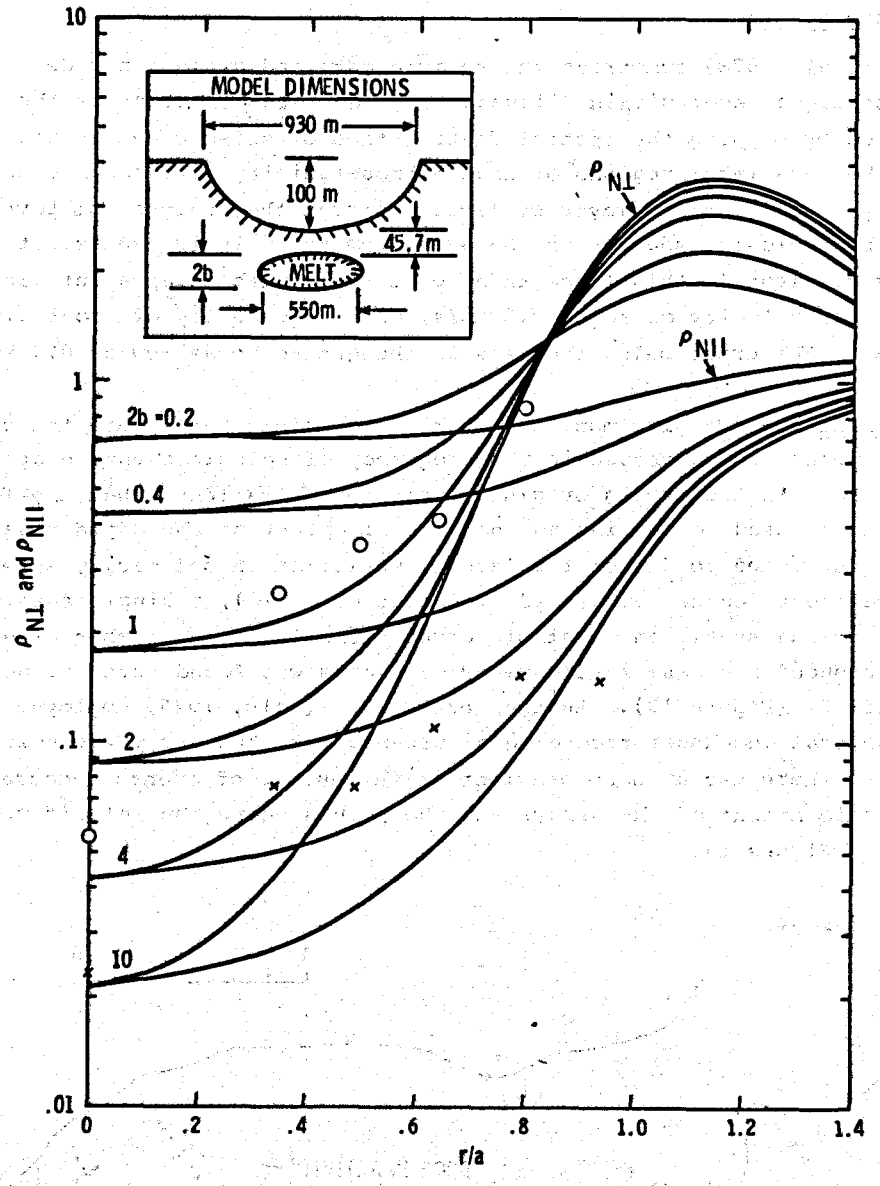

Figure 18. Experimental Data Compared with Calculated Apparent Resistivity Curves for Different Assumed Values of Melt Thickness (after Bostick et al, 1977, Figure 15)

This in itself is an important observation because the telluric field is conveying a great deal of information about the edges of the lava lens as well as about the interface between the molten lens and the surrounding medium. Hence, the telluric field measurements may have provided a significant insight into aspects of the problem which would have had a minimal effect on loop-loop electromagnetic soundings. On the other hand, the loop-loop measurements contributed an estimate of the lens conductance which appears to be far less contaminated by "edge effects." In this sense, the telluric measurements and the loop-loop measurements complement each other very well, each providing information that presents a clearer picture of the physical processes involved.

Seismic Experiments

Aki et al (1978) summarize the seismic data and present a model of the structure of the magma reservoir in Kilauea Iki. The lateral extent of the magma chamber was outlined by mapping the spatial distribution of seismic events within the upper crust of the lava lake; regions of high microseismicity were assumed to be underlaid at depth by a still-molten layer of lava. Through the analysis of Love and P-waves generated by explosive sources and S-waves from teleseismic events, it was concluded that the magma lens is thin (less than 10 metres), with an apparent viscosity of 10^7 poise, a shear velocity of about 0.2 km/s, and a P-velocity of about 0.3 km/s. P-velocity in the crust below the lens is thought to be as low as 0.9 km/s.

Seismicity -- Passive monitoring of microearthquakes within the cooling crust revealed a pronounced decrease in the frequency of seismic events near the edge of the lava lake. If the events originate near the magma lens, then the falloff in activity can be used to outline the horizontal extent of the magma reservoir. Two experiments designed to detect the lateral variation in seismicity were carried out. In one experiment (Chouet et al, 1976; Aki et al, 1978), a single seismograph was placed at various spots, and a simple count was made of the number of events recorded. A pronounced decrease in frequency of events was found north of nail 17N10 and west of nail 22 (Figure 19). Another experiment (Colp, 1976) employed a linear array of several geophones recording simultaneously; the array was shifted to find places where there was a sharp gradient in the number of events recorded across the array. The locations of the arrays and the points where the falloff occurs are indicated in Figure 19.

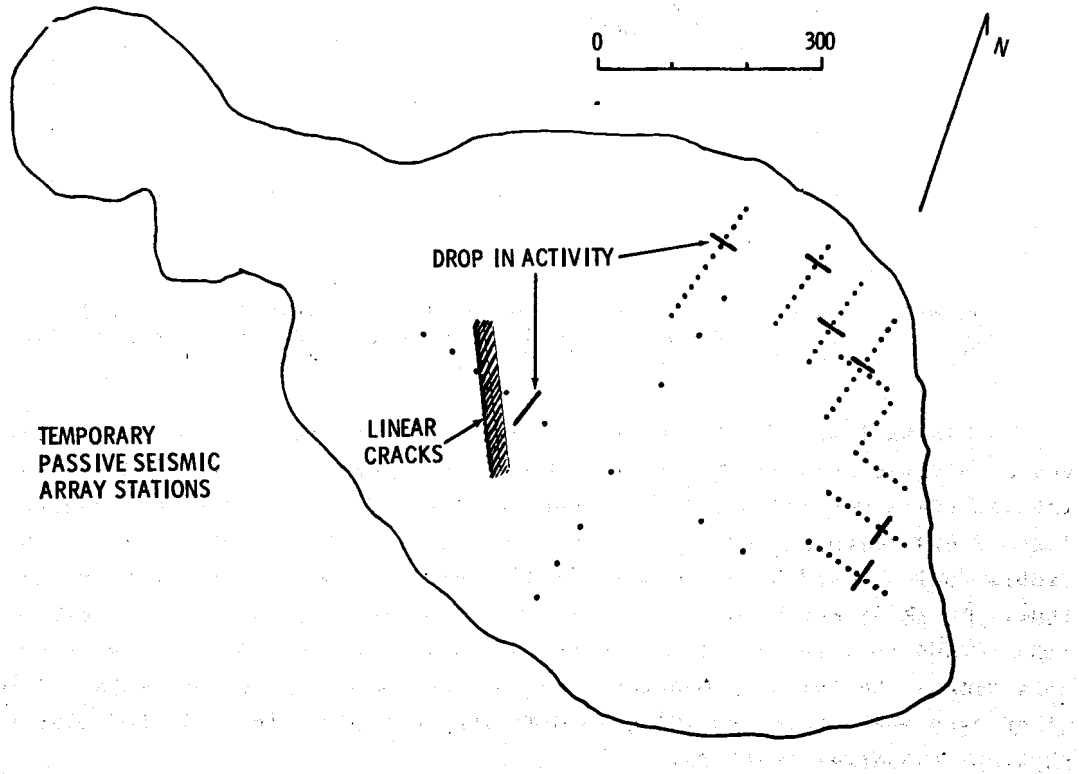

Figure 19. Location of Geophones for Passive Seismic Investigations in Kilauea Iki Lava Lake

On the northern and eastern sides of the lava lake, the gradient in seismicity is located close to the edge of the magma lens as deduced from the electromagnetic experiments (Figure 20). Particle motions of teleseismic P-waves recorded at any array across the northern edge also have the appearance of being diffracted around the edge of a magma lens (Fehler and Aki, 1978). However, the falloff in seismicity to the west of nail 22 lies well within the bounds of the lens determined electromagnetically. Either the edge actually is near nail 22, as the seismicity suggests, or a factor other than the extent of the magma body controls the level of seismic activity, at least locally. We favor the latter explanation.

The microearthquakes are not directly associated with magma; they accompany cracking induced by thermal stresses as the basalt cools and contracts in the temperature range 900°C to ambient (Peck and Minakami, 1968). The amount of cracking may be very sensitive to other factors. Peck and Minakami found a pronounced diurnal variation in the frequency of events over a recording period of 2 months, with a maximum around midnight and a minimum of a factor of 3 smaller around noon. They speculated that expansion and contraction associated with diurnal temperature fluctuations may trigger the growth of preexisting cracks. The amount of cracking is also affected by differential subsidence of the crust of the lake. Although the total subsidence of the surface over the entire lifetime of the lava lens shows a very regular pattern (Figure 21), the history of subsidence is both spatially and temporally nonuniform. In some lava lakes, there are alternating patterns of subsidence and uplift (Wright et al, 1976). In Kilauea Iki, the pattern from September

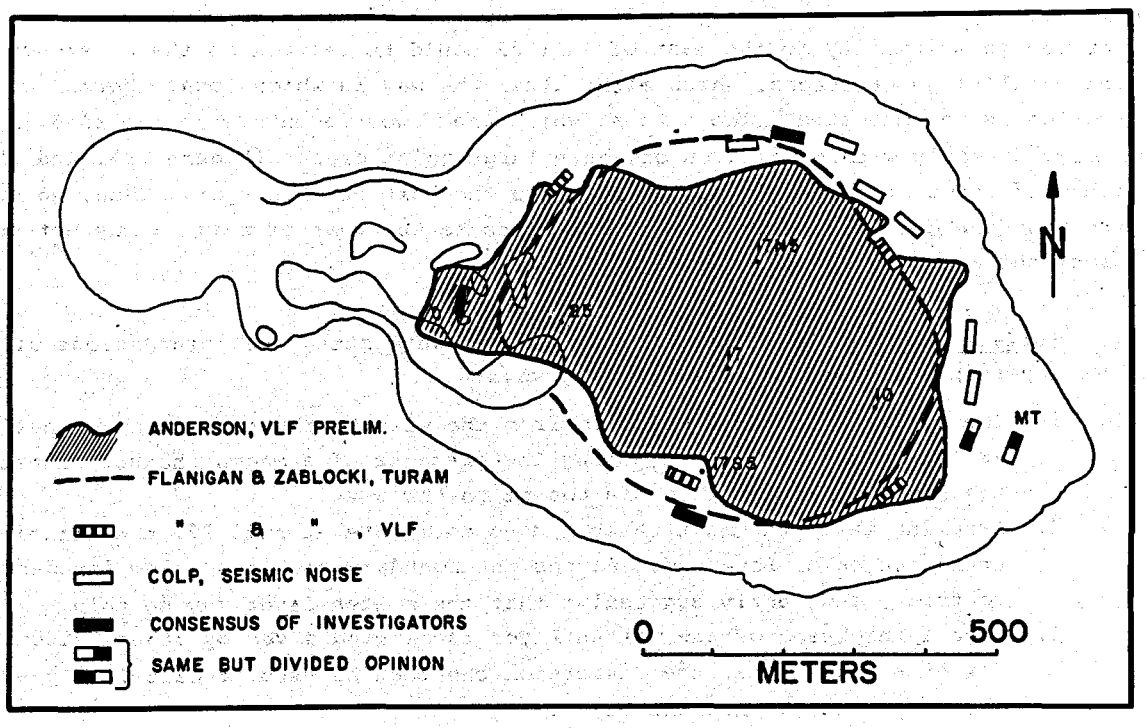

Figure 20. Proposed Lateral Boundary of Molten Lens in Kilauea Iki Lava Lake

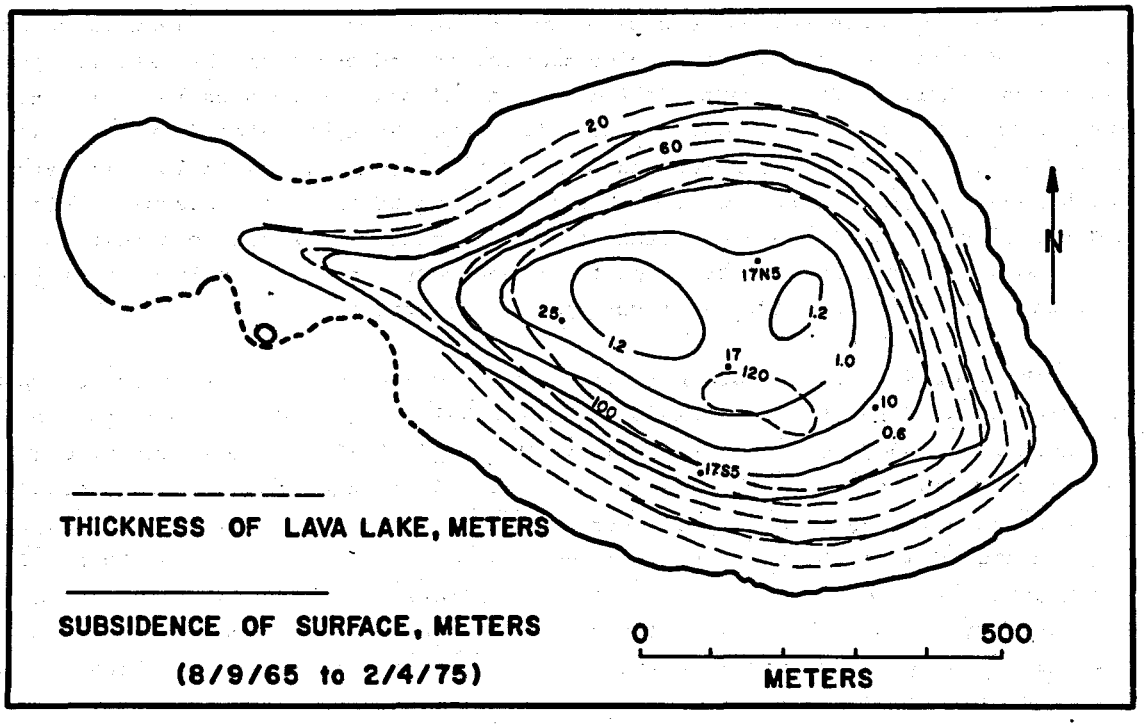

Figure 21. Composite Contour Map of Kilauea Iki Lava Lake, Showing Total Thickness and Subsidence (after Holcomb, 1976)

1964 to August 1965 (Peck and Minakami, 1968) was substantially different from the cumulative pattern shown in Figure 21. The specific factor responsible for the decrease in seismicity to the west of nail 22 could be related to the existence of long parallel joint cracks, which might alter the way in which local thermal contraction is accommodated. The site at which the fewest events were recorded is located directly within the area of these large joint cracks (Figure 19), and the number of events recorded increases again to the west of this spot. Thus, we suggest that the decrease in the number of events to the west of nail 22 may not be be associated with the edge of the magma lens.

Surface Waves -- One of the most important data sets, the observations of Love wave dispersion, is used in three primary ways:

1. The decrease in phase velocity from the west to the east at about nail 22 is cited as evidence suggesting the presence of a magma chamber beneath the eastern section which is absent to the west.
2. Assuming that the magma chamber does terminate at nail 22, the efficient transmission of Love waves across the boundary requires a low impedance contrast, indirectly suggesting that the molten layer may be thin.
3. When a thickness of the molten layer is assumed given by other evidence, Aki et al claim that the dispersion can then be used to calculate the shear velocity within the layer.

Records of Love waves made by transverse horizontal geophones along the major axis of the lava lake show apparent velocity fluctuations along the profile. Some

statistical tests of significance have been applied to the alternate hypotheses that velocity is uniform along the linear array, or that velocity is different in the eastern and western halves of the profile. For the Love waves generated by a shot at the western end of the lake (Figure 10 in Aki et al, 1978), the phase velocity in the eastern half of the profile is significantly slower than the phase velocity in the western half. The exact position of the change in velocity is not well-defined; Aki et al show the change occurring at nail 20, although a change at nail 22 fits the data equally well. A similar profile with a shot at the eastern end of the lake shows no significant difference in velocity. Any real change in velocity is not large enough to appear above the noise level. The difference between the two experiments may be due to the longer predominant periods of the signals in the second experiment. The longer period waves penetrate deeper and may be less sensitive to changes in depth or degree of cracking of the near-surface layers.

The Love waves show normal dispersion, i.e., the phase velocity increases with increasing period. In order to produce a normally dispersed wave in the period range observed, there has to be an increase in shear velocity with increasing depth somewhere in the uppermost 20 to 40 metres of the crust. Presumably, this increase in velocity is caused by a decrease in the amount of cracking with depth.

Love wave data, even covering a much broader frequency range than measured in Kilauea Iki, are notorious for lack of information about the structure. In the period range 0.11 to 0.16 second, Love waves can be expected to supply only one piece of information, sufficient to resolve the velocity but not the thickness of a single layer over a half-space. More layers can be included and are likely to exist, but cannot be resolved. Although Aki et al (1978) acknowledge the non-uniqueness of the inversion, it is worthwhile emphasizing this problem in more detail.

Model A in Figure 22, which is similar to Model A in Figure 11 in Aki et al and which consists of a single layer over a half-space, satisfies the dispersion west of nail 22 reasonably well. East of nail 22, Aki et al modelled the dispersion with four layers over a half-space, including a low-velocity layer immediately above the half-space. Model B in Figure 22 demonstrates that the only change in Model A required to fit the data east of nail 22 is a slight lowering of velocity in the surface layer. Many other minor changes in Model A can also satisfy the data, e.g., an increase in thickness of the surface layer without a decrease in its velocity. With only a minor change in structure from west to east, such as that indicated in Models A and B, the requirement for low impedance contrast between the two structures is automatically satisfied without having to resort to mode conversion or limitations on the thickness of a low-velocity layer. When there is a thick low-velocity channel present, fundamental mode Love waves tend to develop large amplitudes within the channel, thus producing a mismatch in the amplitude-versus-depth functions at the transition to a structure with no low-velocity channel. In this case, as the Love wave entered the zone containing the magma, it would be converted to a higher mode wave which has relatively little amplitude in the channel. Thus, the requirement for a similar amplitude-versus-depth pattern on both sides of nail 22, as discussed by Aki et al, basically means that modes will be selected which are

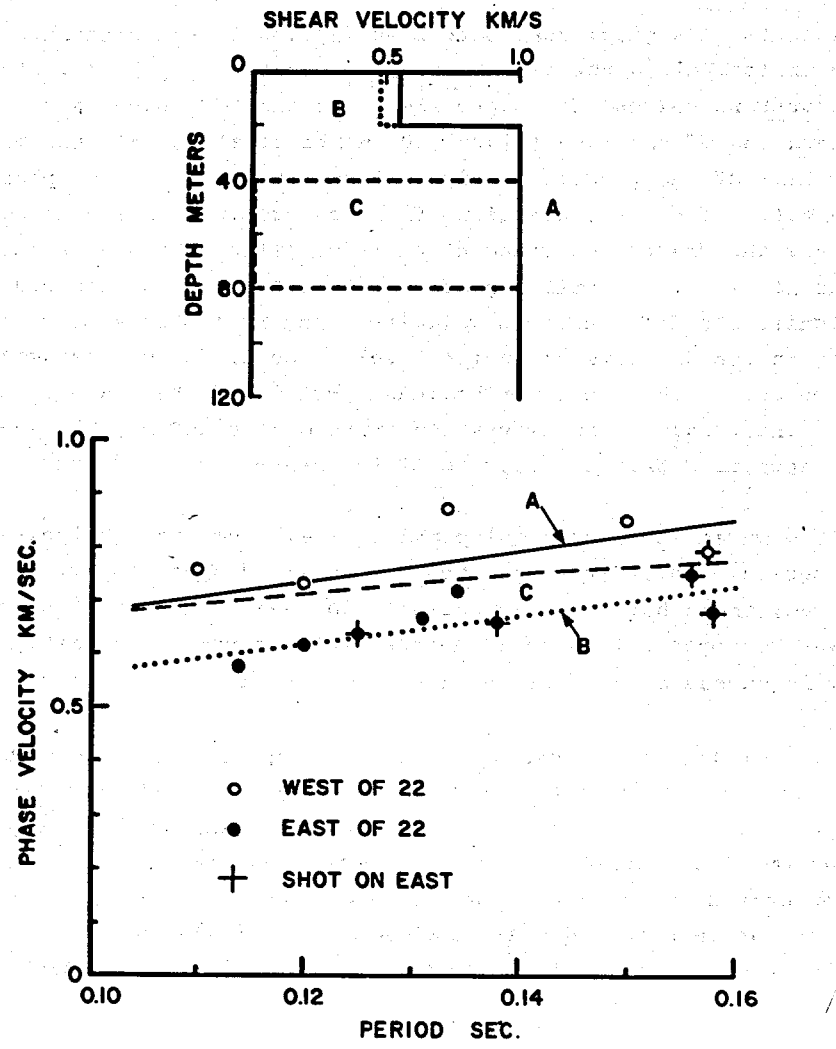

Figure 22. Observed and Theoretical Phase Velocities of Love Waves

insensitive to the channel. Thus, interpretation of the Love wave data does not require the presence of a magma layer beneath either the eastern or the western end of the lake.

On the other hand, the fact that the Love wave data do not require a low-velocity layer does not mean that no such layer exists. Love wave dispersion over a limited frequency range simply is not capable of telling whether a layer is there or not. For example, Model C in Figure 22 differs from Model A in having a liquid layer in which rigidity is reduced to zero. The interface at 40 metres then acts as a free surface for SH-waves. Love wave motion is confined entirely to the upper 40 metres, yet there is very little change in velocity. Slight modifications to Model C could satisfy the data either east or west of nail 22. A low-velocity zone with finite rigidity actually lowers the phase velocity more because then some of the energy can be trapped in the low-velocity zone. The important point is that, by modifying the structure above 40 metres depth, a variety of combinations of low-velocity layer thickness and velocity can be made consistent with the data.

One of the most surprising results of the active seismic experiments is the absence of coherent Rayleigh waves. Why should Love waves be observed when Rayleigh waves are not? Aki et al have suggested that the reason for this may be two-fold. The presence of a thin liquid lava layer could preferentially lower the phase velocity of the Rayleigh waves drastically relative to the Love waves so that the Rayleigh wavelengths would be shortened to such a degree that, relative to Love waves, they would be severely scattered. The second reason suggested by Aki et al is that anisotropy exists in the distribution of cracks. Vertical cracks due to columnar jointing, because they are spaced regularly and uniformly, will affect the elastic moduli of both Rayleigh waves and Love waves equally. On the other hand, horizontal cracks may be distributed irregularly, and, because they affect the shear moduli controlling only the Rayleigh wave mode and not the Love wave mode, Love waves can propagate more coherently.

A third possible explanation is that Love waves are propagating in a layer above and isolated from a liquid, low-velocity layer, as in Model C. Rayleigh waves, however, can propagate within a liquid: much of their energy may be trapped and attenuated within the liquid layer. Because the Love waves may be isolated within surface layers, they provide no information about the molten zone, while the Rayleigh waves which propagate within the zone may be difficult to observe.

Body Waves -- An unexpected result of the passive seismic experiment is the arrival of SH-waves from a teleseismic event, apparently transmitted through the lava lake. Aki et al use this observation to place constraints on the thickness and viscosity of the magma lens. Again, their interpretation is highly nonunique. A naive observer might simply assume that the transmittal of an SH signal, coupled with the fact that the Love wave data can be fit without a low-velocity zone, indicates that there is no molten lens remaining anywhere within the lake. Given the a priori knowledge that such a lens does exist, the arrival of SH-waves becomes an enigma. It was found, however, that a viscosity of the magma on the order of 10^7 poise allows some transmittal of shear energy. With additional assumptions, a transmission coefficient (T) of about 0.014 was found for a 30-metre-thick layer. This transmission coefficient is apparently considered too low. However, a value for T of about 0.03 was calculated for a 10-metre layer and was accepted. A difference factor of 2 when the size of the input signal is not known cannot be considered a satisfactory discriminant.

If T is on the order of 0.03, their model is internally inconsistent. Since most reported values of viscosity for basaltic magmas are in the range 10^3 to 10^5 poise, the authors invoke the Bingham body model of viscosity to justify the viscosity of 10^7 poise needed for transmission of SH-waves. In an experiment by Shaw et al (1968), basaltic magma was found to exhibit a viscosity of 10^3 to 10^4 poise only above a finite yield stress, measured in two cases at 700 and 1,200 dynes/cm^2. Aki et al point out that 10^{-5} cm amplitude of the signal received corresponds to a stress of about 180 dyne/cm^2, well below the yield stress. However, if the transmission coefficient is on the order of 0.03, the incident wave would involve stresses about 33 times larger, well above the yield stress. With a viscous magma, P-waves should also be attenuated. Given the 10-metre layer and a frequency of 10 Hz,

Aki et al compute a transmission coefficient of 0.17 for P-waves. However, a linear array of geophones spread across the northern side of Kilauea Iki found no decrease in amplitude of teleseismic P-waves as far as 100 metres inside the inferred edge of the magma lens (Fehler and Aki, 1978). Also, Aki et al identify late arrivals on refraction records as single and double reflections passing through the molten layer two and four times. If the magma really is unusually viscous and therefore attenuates P-waves, these multiple reflections probably would not be observed. In our opinion, a satisfactory explanation for the apparent arrival of SH-waves has not yet been advanced.

There are a number of plausible alternatives to the Bingham model explanation for the presence of SH-waves. One possibility is that the waves propagate horizontally from the edge nearest the epicenter. Another possibility is that some S-wave energy is converted and transmitted through the magma as a P-wave, then reconverted to an S-wave in the upper crust. This suggestion cannot be lightly dismissed simply because the motion observed was on a transversely oriented geophone. Radial and transverse components were not simultaneously recorded, so the polarization of the wave is not actually known. There could be some SV motion on the transverse geophone if the receivers were not oriented exactly perpendicular to the azimuth to the epicenter, or if the wave did not travel the least-distance path, or if the layering is nonhorizontal, or if the anisotropic orientation of cracks in the upper crust causes the SH- and SV-waves to be coupled. All of these conditions are probably satisfied. Lending credence to this interpretation are the apparent observations of P-wave energy on at least one of the transverse geophones (nail 17S2, Figure 12 in Aki et al, 1978) and the close correlation between transverse and vertical motion during the arrival of the S-wave at another station (nail 17S1). Any mechanism which allowed as much as 10% of the S-wave energy to be received on the transverse geophones would be an order of magnitude more efficient than the transmittal of S-wave energy through a viscous magma lens.

Active seismic refraction experiments were carried out along both the major and minor axes of the lava lake. The first P-arrival is rapidly attenuated with distance and has a very low velocity of only 0.8 to 2.2 km/s. The lowest velocities were found in the highly cracked region near the vent in the westernmost part of the lake. As Aki et al point out, the extremely low velocities must be due to the presence of cracks in the upper crust since the P-velocity of rock samples gives velocities in excess of 4 km/s. The near-surface cracks must also be dry to produce such low velocities.

Determination of P-velocities within and below the presumed magma lens rests on the interpretation of second arrivals on the explosion refraction records. The arrivals were identified as P-waves on the basis of the particle motions on vertical and radial components. Of the records presented (Figures 6 and 7 in Aki et al, 1978), the most convincing correlation between the two components was recorded from shot S1 at nail 17N9, as shown at the top of Figure 23. The vertical and radial components seem to be in phase, indicating P-type particle motion. However, most of the other recordings are much less coherent. In the traces at three successive distances shown in Figure 23, there is great variability in the phase relationships. An equally plausible interpretation of these relatively large-amplitude, long-period

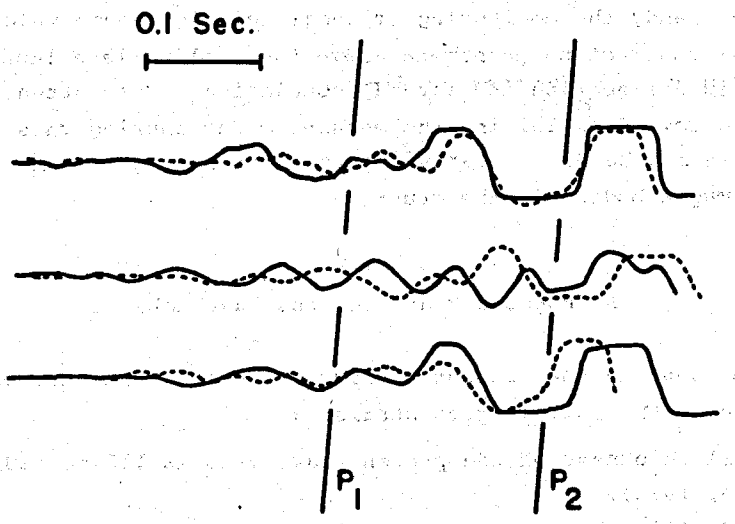

Figure 23. Comparisons of Records From Vertical and Radial Horizontal Geophones (after Aki et al, 1978, Figures 6 and 7). ©American Geophysical Union, 1978. Used by permission.

signals is that they represent the arrival of incoherent Rayleigh wave energy. If more than one Rayleigh mode is present, perhaps one guided primarily within the upper crust and another within a low-velocity channel, their interference could produce the pronounced phase and amplitude variability which is observed. The interference of two modes could also be another explanation for the unusual lack of coherent Rayleigh waves noted earlier.

If the identification of the later arrivals as P-waves is correct, the interpretation in terms of velocity structure rests on two weak points: the delay time $\Delta\tau$ and the thickness of the low-velocity layer. The onset of the signal is not at all clear (see Figure 23 in this report and Figures 6 and 7 in Aki et al). The peak preceding the preferred arrival time on most of the horizontal records could equally well have been chosen and would reduce $\Delta\tau$ by 30% or more. As discussed previously, constraints on the thickness of the low-velocity zone are very weak. By assuming a thin molten layer, the authors are forced to accept both very low P-velocity within the magma and low velocities in the crust beneath the lens.

Summary of Seismic Experiments -- The resolution of the seismic experiments was limited by the difficult environment. Attenuation and scattering within the cracked crust and possibly within the magma itself severely curtail the range in which clear signals can be received in an active experiment. The primary information gained from P-waves and Love waves in the active experiments concerns the nature and extent of cracking in the uppermost crust. The fortuitous reception of teleseismic signals provided some additional constraints on the structure of the lava lake, but the interpretation is uncertain without more precise control from active experiments. None of the seismic experiments provides unequivocal evidence that a molten reservoir even exists; given that it does exist, there is very little control on its thickness or lateral extent.

On the other hand, the monitoring of local seismic events which are apparently related to thermal contraction phenomena above the cooling lava lens has proven to be a useful tool in delineating its lateral boundaries. More attention, however, should be directed toward explaining the mechanism for causing this impulsive seismic activity. This may be particularly important if analog phenomena are associated with large-scale magma bodies in the crust.

A Proposed Model for the Lava Lake

A model representing the present configuration and structure of Kilauea Iki lava lake must embody the following constraints:

1. The total thickness of the present lava lake is 115 to 120 metres (Holcomb, 1976).
2. Recent drilling has encountered melt at a depth of 45 metres; however, it was not possible to penetrate the melt more than 0.5 metre (Colp and Okamura, 1978).
3. Temperature logs in recent drill holes reveal isothermal temperatures of 100°C from 10 metres depth to 33 metres, where a rapid increase in temperature occurs until melt (probably 1,070 $\pm$ 5°C) is encountered at 45 metres (Colp, 1976).
4. Schlumberger electrical sounding data define a very resistive surface layer 5 metres thick and a wet, less resistive, warm layer at 5 metres, extending to approximately 30 metres, underlaid by a very resistive layer representing the top of the transition zone between 100°C and 1,070°C (Zablocki, 1976; Smith et al, 1977).
5. Love wave dispersion indicates the amount of cracking must decrease with depth. The very low P-wave velocities require the cracks to be dry, at least in the uppermost crust (Aki et al, 1978).
6. Two-loop electromagnetic sounding data reveal a layer at a depth of 38 to 44 metres having a total conductance of 6.86 mhos.
7. Field studies on the petrology of the prehistoric Makaopuhi lava lake, in conjunction with thermal history calculations, suggest that maximum temperatures and the slowest rate of cooling are encountered in a depth range slightly below the middle of the lava lake, at a depth from 54% to 60% of the total lake thickness (Evans and Moore, 1968).

A proposed model meeting these constraints is shown in Figure 24, along with the geological model of Smith et al (1977). Since the gravitational settling of olivine crystals and the upward migration of residual fluid eventually forming glass are useful indicators of rheological and temperature conditions in the melt at intermediate times in the cooling history of the lava layer, the authors have also

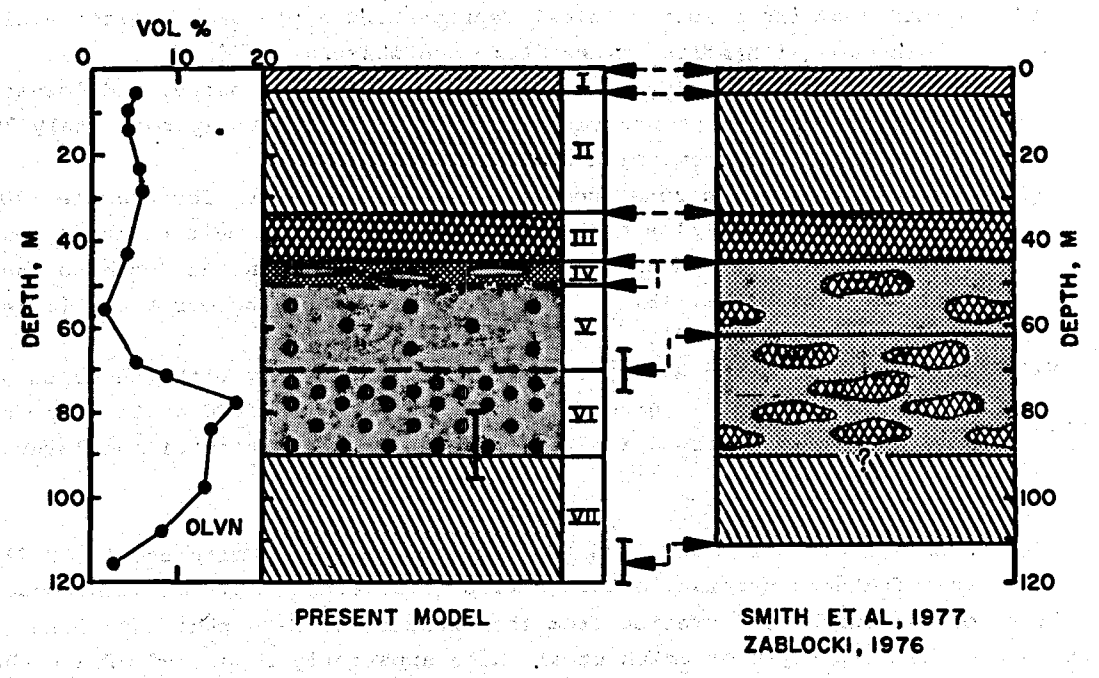

Figure 24. Proposed Model of Vertical Section through Kilauea Iki Lave Lake

shown smoothed versions of the concentrations of olivine phenocrysts and residual glasses as observed by Moore and Evans (1967) on the prehistoric Makaopuhi lava lake. Since the prehistoric lava lake had a depth of 67 metres and the present Kilauea Iki lava lake has a depth of 115 to 120 metres, the authors have simply expanded the depth scale of Moore and Evans by a linear factor of 115/67. Smoothing of the original data was accomplished using visual three-point averages.

Although conceivably the depths shown in Figure 24 should have been arrived at by expanding the original depths according to some rigorous scaling law, the fact is the authors are not certain what the scaling law would be for this complex situation, nor is it known, with any degree of certainty, that the initial conditions were at all analogous between the Makaopuhi prehistoric flow and the present-day Kilauea Iki lava lake. The authors feel that a linear scaling factor is the most sophisticated that should be used in light of the uncertainties involved.

The model in Figure 24 has the following layers:

I. A dry, resistive surface layer from the surface to approximately 5 metres (Zablocki, 1976).

II. A warm, wet layer at 100°C, containing appreciable water and/or steam from 5 metres to a depth of 33 metres (Zablocki, 1976).

III. A transition layer from 33 to 45 metres over which temperatures increase from 100° to 1,070°C. The top of this layer will appear resistive as water is flashed as superheated steam; the bottom will appear conductive as temperatures become sufficiently high to activate appreciable conduction in the rock itself (Zablocki, 1976; Smith et al, 1977). Layers IV, V, and VI are all in the so-called melt zone.

IV. A thin zone (to 5 metres thick) representing a plexus of molten sills interbedded with solid layers (Colp and Okamura, 1978).

V. A layer having the highest temperature, lowest viscosity, and lowest density of olivine phenocrysts from 49 $\pm$ 2 metres to approximately 70 metres (modified from Smith et al, 1977).

VI. A smooth transition zone from low-viscosity melt at, for example, 70 metres to a crystalline mush, and then into cooler melt having a lower density of olivine phenocrysts. The uncertainty in the depth to the bottom of this layer (87 $\pm$ 7 metres) is shown by the error bar (after Moore and Evans, 1967).

VII. Solid basalt having a temperature which, in analogy with the calculation of Shaw et al (1977), gradually decreases from 1 070°C at the top of the layer (80 to 95 metres) to 700° or 750°C at the bottom of the layer (115 to 120 metres).

A comparison of this model with the previous model of Smith et al (1977) shows that the gross features persist, although minor differences have been introduced in the light of geological information from the prehistoric Makaopuhi lava lake. In particular, the melt layer of Smith et al which apparently consisted of a rather uniform distribution of large solid blocks of more refractory material is replaced by Layers IV and V of Figure 24. Layer V is somewhat thicker than the electrically active zone of Smith et al and, unlike the active zone of Smith et al, is not underlaid abruptly by a layer 100 times more resistive but instead grades smoothly, both electrically and rheologically, into a crystalline mush.

The difference in total thickness between the two models is of little consequence, since the 111-metre thickness used by Smith et al is based on an older published value probably representing an average thickness for the entire lake, and our 115- to 120-metre thickness represents a recent evaluation by Holcomb (1976) of the total thickness in the deepest part of the lake.*

The Lateral Boundaries of the Lava Lens

Both active electromagnetic experiments and the passive monitoring of local seismic events have served to define the lateral boundaries of the lava lens. In particular, the Turam and VLF investigations of Flanigan and Zablocki (1977), along with additional preliminary VLF data furnished by L. Anderson (1976), have been useful electromagnetic techniques in this phase of the study.

The monitoring of impulsive natural seismic events was initiated by K. Aki and B. Chouet (Chouet et al, 1976) and continued by Colp (1976b).

*Drilling in the lava lake by Sandia in 1978 and 1979 confirmed the basic elements of this proposed vertical model, in particular, the existence of the crystalline mush. The thickness of the molten layer having a low concentration of olivine phenocrysts may have been somewhat overestimated.

A map (Figure 20) showing the boundary of the lava lens as determined by all of these workers shows excellent agreement between the various methods on the northern and eastern sides and suggests that uncertainty regarding the precise location of the edge of the lens lies within a band from 25 to 50 metres wide. However, there is fundamental disagreement between the seismic and electromagnetic methods on the location of the western edge of the lens. It may be that there is only a very thin lens west of nail 22 which can be detected electromagnetically but is transparent to seismic techniques. This question can probably be answered only by a drilling program. The minimum diameter of the lava lens is 500 metres north-south, and the maximum diameter is 750 metres east-west. Moreover, the audio magnetotelluric investigations of Bostick et al (1977) suggest that the entire lava lens is enveloped by a water-depleted steam sheath.

Speculation on the Thickest Portion of the Lava Lens -- The geophysical sensing experiments to date have only obliquely suggested lateral variations in either the material characteristics or the thickness of the lava lens. At present it is felt that the best constraints on where the lava lens is thickest are provided by the maximum total thickness of the entire lava lake, as derived from subtracting preflow topography from present topography, and the area of maximum subsidence of the surface due to thermal contraction and crystallization of the lava upon cooling.

In Figure 21 is a composite contour map in which the total lake thickness and the surface subsidence data of Holcomb (1976) are compared. From this comparison it is suspected that the melt would have a relatively uniform maximum thickness over an area 300 metres wide and 500 metres long, centered approximately on nail 17N2.

In summary, it is felt that the geophysical sensing experiments on Kilauea Iki lava lake have provided a unique opportunity to quantitatively define the configuration and structure of a small-scale active magma body. Although in this report a great deal of attention has been paid to assessing the strengths and weaknesses of the various methods and experimental results, the end product of all these experiments should illustrate the value in closely coordinating comprehensive geophysical and geological investigations of active magma systems. In this respect, the project can be regarded as being overwhelmingly successful.

Bibliography

Aki, K., B. Chouet, M. Fehler, G. Zandt, R. Koyanagi, J. Colp, and R. G. Hay, Seismic properties of a shallow magma reservoir in Kilauea Iki by active and passive experiments, JGR, 83, 2273-2282, 1978.

Anderson, L., Private communication of preliminary VLF data to John Colp, 1976.

Bostick, F. X., H. W. Smith, and J. E. Boehl, Audio Magnetotelluric Measurements on Kileuea Iki Lava Lake, Final Report to Sandia Laboratory, Albuquerque, NM, 1977.

Chouet, B., K. Aki, and G. Zandt, Mapping a magma reservoir by locating thermal cracks (ab.) AGU Fall Meeting Program, 1976.

Colp, John, Magma Energy Research Progress Report, Sandia Laboratories, Albuquerque, NM, 1976.

Colp, J., A fine-mesh passive seismic survey of Kilauea Iki Lava Lake (abs.) AGU Fall Meeting Program, 1976.

Colp, J. L., R. W. Decker, J. F. Hermance, D. L. Peck and P. L. Ward, Magma Workshop Assessments and Recommendations, Sandia Laboratories Energy Report, SAND75-0306, 44 pp., 1975.

Colp, J. L. and Okamura, R., Drilling Into Molten Rock at Kilauea Iki, Transactions, Geothermal Resources Council, Vol. 2, July 1978.

Evans, B. W., and J. G. Moore, Mineralogy as a function of depth in the prehistoric Makaopuhi tholeiitic lava lake, Hawaii, Contr. Mineral. Petrol., 17, 85-115, 1968.

Fehler, M. and K. Aki, Numerical study of diffraction of plane elastic waves by a finite crack with application to location of a magma lens, Bull. Seism. Soc. Amer., 68, 573-598, 1978.

Flanigan, V. J., and C. J. Zablocki, Mapping the lateral boundaries of a cooling basaltic lava lake, Kilauea Iki, Hawaii, USGS Open-File Report 77-94, 21 pp., 1977.

Frischknect, F. C., Private Communication, 1976.

Frischknect, F. C., Electromagnetic scale modelling. In Electromagnetic Probing in Geophysics (J. R. Wait, ed.), pp. 265-318, Golem Press, Boulder, CO, 1971.

Grant, F. S. and G. F. West, Interpretation Theory in Applied Geophysics, 564 pp., McGraw-Hill, New York, 1965.

Holcomb, Robin, Private communication of lava lake thickness and surface subsidence to John Colp, 1976.

Khitarov, N. I. and A. B. Slutskiy, 1965, The effect of pressure on the melting temperatures of albite and basalt (based on electroconductivity measurements): Geochem. Int., v. 2, pp. 1034-1042.

Khitarov, N. I., A. B. Slutskiy and V. A. Pugin, Electrical conductivity of basalts at high T-P and phase transitions under upper mantle conditions, Phys. Earth Planet. Interiors, 3, pp. 334-342, 1970.

Moore, J. G. and B. W. Evans, The role of olivine in the crystallization of the prehistoric Makaopuhi tholeiitic lava lake, Hawaii, Contr. Mineral. Petrol., 15, 202-223, 1967.

Murase, T., and A. R. McBirney, Properties of some common igneous rocks and their melts at high temperatures, Geol. Soc. Am. Bull, 84, pp. 3563-3592, 1973.

Murata, K. J., An acid fumarolic gas from Kilauea Iki, Hawaii, U.S. Geological Survey Prof. Pap., 537-C, 61-66, 1966.

Murata, K. J., and D. H. Richter, Chemistry of the lavas of the 1959-60 eruption of Kilauea volcano, Hawaii, U.S. Geol. Surv. Prof. Pap., 537-A, 26 pp., 1966a.

Murata, K. J., and D. H. Richter, The settling of olivine in Kilauean magma as shown by lavas of the 1959 eruption, Amer. J. Sci., Ser. 4, 264, 194-203, 1966b.

Peck, D. L., Lava coils of some recent historic flows, Hawaii, in Geological Survey Research 1966, U.S. Geol. Surv. Prof. Pap., 550-B, B148-B151, 1966.

Peck, D. L., Density of molten lava in Alae lava lake, Hawaii (abstract), Trans. AGU, 50, 339, 1969.

Peck, D. L., Thermal properties of basaltic magma; results and practical experience from study of Hawaiian lava lakes, in the Utilization of Volcano Energy, edited by J. L. Colp and A. S. Furumoto, pp. 287-298, Sandia Laboratories, Albuquerque, New Mexico, 1974.

Peck, D. L., and W. T. Kinoshita, The eruption of August, 1963 and the formation of Alae lava lake, Hawaii, U.S. Geol. Surv. Prof. Pap., in press.

Peck, D. L. and T. Minakami, The formation of columnar joints in the upper part of Kilauean lava lakes, Hawaii, Geol. Soc. Amer. Bull., 79, 1151-1166, 1968.

Peck, D. L., J. G. Moore, and G. Kojima, Temperatures in the crust and melt of Alae lava lake, Hawaii, after the August 1963 eruption of Kilauea volcano-a preliminary report, in Geological Survey Research 1964, U.S. Geol. Surv. Prof. Pap., 501-D, D1-D7, 1964.

Peck, D. L., T. L. Wright, and J. G. Moore, Crystallization of tholeiitic basalt lava in Alae lava lake, Hawaii, Bull. Volcanol., 29, 629-656, 1966.

Peck, D. L., M. S. Hamilton, and H. R. Shaw, Numerical analysis of lava lake cooling models: Part II, Application to Alae lava lake, Hawaii, Am. Jour. Sci., 277, 415-437, 1977.

Presnall, D. C., C. L. Simmons, and H. Porath, Changes in electrical conductivity of a synthetic basalt during melting, JGR, 77, pp. 5065-5073, 1972.

Richter, D. H., and J. G. Moore, Petrology of the Kilauea Iki lava lake, Hawaii, U.S. Geol. Surv. Prof. Pap., 537-B, 26 pp., 1966.

Richter, D. H., and K. J. Murata, Petrography of the lavas of the 1959-60 eruption of Kilauea volcano, Hawaii, U.S. Geol. Surv. Prof. Pap., 537-D, 12 pp., 1966.

Richter, D. H., J. P. Eaton, K. J. Murata, W. U. Ault, and H. L. Krivoy, Chronological narrative of the 1959-60 eruption of Kilauea volcano, Hawaii, U.S. Geol. Surv. Prof. Pap., 537-E, E1-E73, 1970.

Shaw, H. R., T. L. Wright, D. L. Peck, and R. Okamura, The viscosity of basaltic magma: An analysis of field measurements in Makaopuhi lava lake, Hawaii, Amer. J. Sci., 226, 225-264, 1968.

Shaw, H. R., M. S. Hamilton, and D. L. Peck, Numerical analysis of lava lake cooling models: Part I, Description of the method, Am. Journ. Sci, 277, 384-414, 1977.

Smith, B. D., C. J. Zablocki, F. C. Frischknect and V. J. Flanigan, Summary of results from electromagnetic and galvanic soundings on Kilauea Iki lava lake, USGS Open File Report 77-59, 27 pp., 1977.

Strangway, D. W., Electromagnetic scale modelling. In Methods and Techniques in Geophysics (S. K. Runcorn, ed.), 2, pp. 1-31, Interscience, New York, 1966.

Watanobe, H., Measurements of electrical conductivity of basalt at temperatures up to 1500° C and pressures to about 20 kilobars, Special Contrib., Geophysical Institute, Kyoto Univ., 10, p. 159-170, 1970.

Wright, T. L., D. L. Peck, and H. R. Shaw, Kilauea lava lakes: natural laboratories for study of cooling, crystallization and differentiation of basaltic magma, Chapter 32 in The Geophysics of the Pacific Ocean Basin and its Margin, Geophysical Monograph 19, edited by G. H. Sutton, M. H. Manghnani, R. Moberly, pp. 375-390, American Geophysical Union, Washington, DC, 1976.

Zablocki, C., Some electrical and magnetic studies on Kilauea Iki lava lake, Hawaii, USGS Open-File Report 76-304, 19 pp., 1976.

DISTRIBUTION:

DOE/TIC-4500-R67 UC-66 (224)

Massachusetts Institute of
of Technology
Dept of Earth Science
Cambridge, MA 02139
Attn: Keiiti Aki, 54-526

Lawrence Berkeley Laboratory (3)
University of California
Berkeley, CA 94720
Attn: J. A. Apps
I. S. Carmichael
P. A. Witherspoon

Shigeo Aramaki
Earthquake Research Inst
University of Tokyo
Bunkyo-ku
Tokyo 113, Japan

University of California
Lawrence Livermore Laboratory
P.O. Box 808
Livermore, CA 94550
Attn: R. Austin, Proj Leader -
Geothermal Program

US Department of Energy (2)
Div of Geothermal Energy
Washington, DC 20545
Attn: C. Carwile, Chief
Adv Tech Br
J. W. Salisbury
Hydrothermal Support Br

Sveinbjorn Bjornsson
Science Institute
University of Iceland
Bunhaga 3
107 Reykjavik, Iceland

Argonne National Laboratory
9700 South Cass Avenue
Argonne, IL 60439
Attn: M. Blander, Bldg 205

Office of Nucl and Energy Tech Affairs
Department of State
Washington, DC 20520
Attn: J. L. Bloom

Oregon State University
Corvallis, OR 97331
Attn: G. Bodvarsson

University of Texas
Engineering - Sci Bldg 623
Austin, TX 78712
Attn: F. X. Bostick

Stanford University
Petroleum Eng Dept
Stanford, CA 94306
Attn: W. E. Brigham

Los Alamos Scientific Lab (6)
P.O. Box 1663
Los Alamos, NM 87545
Attn R. Brownlee, G-DO, MS 570
C. E. Holley, CNC-2, MS 738
A. W. Laughlin, G-6, MS 978
R. E. Reicker, G-DOT, MS 26
M. C. Smith, G-DOT, MS 26
C. Herrick, CMB-8

State Univ of NY at Albany
ES 215
1400 Washington Ave
Albany, NY 12222
Attn: K. Burke

US Geological Survey (6)
345 Middlefield Road
Menlo Park, CA 94025
Attn: R. Christiansen
W. A. Duffield, MS 18
J. G. Moore
D. W. Peterson, MS 26
H. Shaw, MS 18
P. Ward

US Geological Survey
Hawaiian Volcano Observatory
Hawaii Volcanoes National Park
Hawaii 96718
Attn: R. W. Decker

University of Texas
Center for Energy Studies
Austin, TX 78712
Attn: M. Dorfman

US Geological Survey (5)
956 National Center
Reston, VA 22092
Attn: G. Eaton, MS 911
R. T. Helz, MS 959
D. Peck, Chief
Geologist, MS 911
R. Tilling, MS 906
C. Zablocki, MS 906

Ingvar B. Fridleifsson
National Energy Authority
Laugavegur 116
Reykjavik, Iceland

Texas A&M University
Center for Tectonophysics
College Station, TX 77843
Attn: M. Friedman

DISTRIBUTION (cont):

US Geological Survey
Box 25046
Denver Federal Center
Denver, CO 80225
Attn: F. Frischknecht, MS 964

University of Hawaii (3)
Hawaii Inst of Geophysics
Honolulu, HI 96822
Attn: C. Helsley, Head
M. Ryan
A. S. Furumoto

Brown University
Dept of Geological Sciences
Providence, RI 02912
Attn: J. F. Hermance

Stanford University
Geology Dept
Stanford, CA 94305
Attn: R. Holcomb

C. A. Kezar
Technical Consultant
Subcommittee on Adv Energy
and Technologies
House Committee on Science
and Technology
Rayburn Office Bldg B374
Washington, DC 20515

University of Alaska
Geophysical Institute
Fairbanks, AK 99701
Attn: J. Kienle

US Dept of Energy (11)
Office of Basic Energy Science
Washington, DC 20545
Attn: G. A. Kolstad, MS J-309 (10)
I. MacGregor, MS J-309

Oak Ridge National Lab
P.O. Box X
Oak Ridge, TN 37830
Attn: W. L. Marshall

Kazuaki Nakamura
Earthquake Research Inst
University of Tokyo
Hongo
Tokyo 113, Japan

Hans-Ulrich Schmincke
Rohr-Universitat Bochum
Institut fur Mineralogie
D-463 Bochum Postfach 102148
West Germany

University of California, Los Angeles
School of Engineering and Applied Science
Materials Department
Los Angeles, CA 90024
Attn: D. L. Douglass

Daisuke Shimozuru
Earthquake Research Institute
University of Tokyo
Bunkyo-ku
Tokyo 113, Japan

University of Hawaii at Manoa
College of Engineering
Honolulu, HI 96822
Attn: Dean John Shupe

University of Minnesota
Inst of Technology
107 Lind Hall
207 Church St SE
Minneapolis, MN 55455
Attn: Dean Roger Staehle

Dartmouth College
Dept of Earth Science
Hanover, NH 03755
Attn: R. E. Stoiber

Superintendent
Hawaii Volcanoes Natl Park
Hawaii 96718

University of Hawaii
Hawaii Geothermal Project
240 Holmes Hall
2540 Dole St
Honolulu, HI 96822
Attn: P. C. Yuen

Dr. Richard Taschek
2035 47th St
Los Alamos, NM 87544

4000 A. Narath*
4700 J. H. Scott*
4710 G. E. Brandvold*
4720 V. L. Dugan*
4730 H. M. Stoller*
4732 D. A. Northrop*
4733 C. L. Schuster*
4734 A. L. Stevens*
4734 R. R. Neel*
4737 B. E. Bader*
4740 R. K. Traeger*
4741 S. G. Varnado*
4742 A. F. Veneruso*
4743 H. C. Hardee
4743 J. L. Colp (30)

DISTRIBUTION (cont):

4743	J. C. Dunn*
5000	J. K. Galt*
5500	O. E. Jones*
5510	D. B. Hayes*
5513	D. W. Larson
5520	T. B. Lane*
5521	S. N. Burchett
5541	W. C. Luth
5541	T. M. Gerlach
5800	R. S. Claassen*
5820	R. E. Whan*
5822	E. J. Graeber
5830	M. J. Davis
5836	J. L. Ledman
8266	E. A. Aas
3141	T. L. Werner (5)
3151	W. L. Garner (3)
	For DOE/TIC (Unlimited Release)

*To receive abstract only.